Subcommission on Silurian Stratigraphy

Formal proposal for a new Global Boundary Stratotype Section and Point (GSSP) for the Aeronian Stage at Hlásná Třebaň, Czech Republic



Formal proposal for a new Global Boundary Stratotype Section and Point (GSSP) for the Aeronian Stage at Hlásná Třebaň, Czech Republic

Petr Štorch¹, Štěpán Manda², Jakub Vodička³, Anthony Butcher⁴, Zuzana Tasáryová², Jiří Frýda², Leona Chadimová¹ and Michael J. Melchin⁵

Abstract: The lowest occurrence of the planktic graptolite *Demirastrites triangulatus* Harkness, 1.38 m above the base of the black shale succession of the Želkovice Formation at the Hlásná Třebaň section in central Bohemia (Czech Republic), is proposed to mark the base of the Aeronian Stage of the Silurian System. The section, fulfils all formal requirements for stratotype of a chronostratigraphic unit. It is proposed as a new Global Stratotype Section and Point (GSSP) to replace the existing, inadequate stratotype in the Trefawr track cutting in the northern Llandovery area of Wales. An abundant, well-preserved, high-diversity graptolite fauna in the section occurs in association with common, although less stratigraphically significant chitinozoans, consistent with the Spinachitina maennili Biozone. The section comprises the lower-middle Aeronian (Dem. triangulatus-Lituigraptus convolutus graptolite biozones) together with the underlying Rhuddanian (Akidograptus ascensus-Coronograptus cyphus biozones) and Hirnantian strata. Several graptolite genera of primary importance in global correlation (Demirastrites, Petalolithus, Rastrites and Campograptus) have their lowest occurrences in the lower part of the triangulatus Biozone and several key taxa indicative of the cyphus Biozone have their last appearance at or near the proposed level of the GSSP, helping to further constrain the level for precise international correlation. The structurally simple black shale succession is somewhat condensed but the boundary interval is within uniform black shale without any sign of disconformity. The C_{org} isotope record exhibits a minor but globally correlatable positive excursion (the Early Aeronian Carbon Isotope Excursion/EACIE) just above the base of the triangulatus Biozone, whereas the TOC and N isotope records indicate uninterrupted sedimentation under stable, anoxic settings. The section can be correlated precisely with sections in Wales, the original type area for the Aeronian, and preserves the intended biostratigraphic datum for the definition of Aeronian Stage. Long-term preservation of this easily accessible section is secured by its location in Bohemian Karst Protected Landscape area.

¹Petr Štorch [storch@gli.cas.cz] and Leona Chadimová [chadimova@gli.cas.cz], Institute of Geology CAS, Rozvojová 269, 165 00, Praha 6, Czech Republic;

²Štěpán Manda [stepan.manda@geology.cz], Zuzana Tasáryová [zuzana.tasaryova@geology.cz] and Jiří Frýda [bellerophon@seznam.cz], Czech Geological Survey, Klárov 3 118 21, Praha 1, Czech Republic;

³ Jakub Vodička [psoqvl@seznam.cz], Bohemian Karst Museum, Husovo náměstí 87, 266 01, Beroun, Czech Republic.

⁴Anthony Butcher [anthony.butcher@port.ac.uk] University of Portsmouth, Burnaby Road, Portsmouth PO1 3QL, U.K.

⁵Michael J. Melchin [mmelchin@stfx.ca], St. Francis Xavier University, Antigonish, Nova Scotia, Canada B2G 2W5.

1. Introduction

The Silurian System was the first Palaeozoic System for which all boundary stratotypes of its component series and stages were formally established during the 1980s (Holland & Bassett 1989). With a single exception, all of the stratotypes were selected in the classic Palaeozoic locations in Great Britain. However, subsequent progress in high-resolution stratigraphy and correlation has revealed serious flaws in some of these early-defined stratotypes (e.g., Melchin *et al.*, 2004). During its Field Meeting held in Ludlow, U.K. in 2011 the International Subcommission on Silurian Stratigraphy (ISSS) visited the boundary stratotypes of the Silurian series and stages in Wales and England (Ray 2011) and found that several of the GSSPs did not meet current requirements for resolution in global correlation. A unanimous decision was made to search for better GSSPs and replace the present inadequate stratotypes. Two working groups were formally established by the ISSS to search for new basal stratotypes for the Aeronian and Telychian stages of the Llandovery Series.

Global correlation of offshore marine Silurian rocks relies primarily on planktic graptolites, supplemented by organic-walled microfossils (namely chitinozoans), and conodonts, which are commonly confined to limestone successions. Biostratigraphic correlation has been reinforced by chemostratigraphy, particularly carbon isotope chemostratigraphy (Melchin & Holmden 2006; Cramer et al. 2011 a.o.). Planktic graptolites are the most common and stratigraphically important fossils to be found in anoxic black shales, which predominate in many Rhuddanian and Aeronian offshore sedimentary successions worldwide. It has been proposed that widespread black shale sedimentation in the Rhuddanian resulted from the Hirnantian deglaciation of the southern hemisphere, with concomitant global warming, a rapid rise of sea-level, and temporary decline in the rate of deep oceanic circulation (Melchin et al. 2013). At that time, graptolitic shales spread globally over all latitudes in which sedimentary successions are preserved and at a wide range of water depths, whereas limestone deposition was confined to the shallower, more in-shore areas of deeply flooded shelves and platforms. Although lowermost Silurian strata - Rhuddanian and Aeronian – have been recognized in many Palaeozoic terrains around the globe, readily accessible Rhuddanian-Aeronian boundary sections without a break in sedimentation or significant lithological change that are rich in well-preserved graptolites are relatively few and for the most part limited to Europe and China. Largely uninterrupted off-shore black shale successions with prolific planktic graptolites are particularly widespread in the lower Silurian of peri-Gondwanan Europe.

We have examined the correlative potential of the Rhuddanian-Aeronian boundary sections in the classical lower Palaeozoic succession of the Prague Synform in the Barrandian area of central Bohemia. Graptolite biostratigraphy was integrated with the chitinozoan fossil record, and organic carbon and nitrogen isotope geochemistry to maximize the correlation potential of the section. The Hlásná Třebaň section matches the formal requirements for a boundary stratotype (see Salvador 1994) and is proposed herein as a replacement for the current Aeronian GSSP in the Trefawr track cutting in Wales, U.K. (see Melchin *et al.* 2020 for a recent review). A detailed lithological log of the Hlásná Třebaň section was made and a variety of geochemical and rock magnetic proxies were examined to assess the depositional and palaeoredox conditions and palaeoproductivity across the broad Rhuddanian-Aeronian boundary interval in the studied section.

2. Present GSSP of the Aeronian Stage

The Aeronian was first defined as a stage by Cocks *et al.* (1984), who derived the name from the Cwm-coed-Aeron Farm located *c.* 500 m from the base Aeronian GSSP in the Trefawr track cutting in the northern part of the type Llandovery area of Wales. The Rhuddanian-Aeronian boundary occurs within the Cefngarreg Sandstone Formation – a *c.* 25 m thick tongue of muddy sandstones within Trefawr Formation (Cocks *et al.* 1984; Davies *et al.* 2010). Sparsely occurring graptolites allow for tentative recognition of *Pernerograptus revolutus* (or *Coronograptus cyphus*), *Demirastrites triangulatus* and *Neodiplograptus magnus* (or *Demirastrites pectinatus*) Biozone assemblages. Along with the graptolites, chitinozoans of the *Spinachitina maennili* Biozone are represented, and brachiopods occur intermittantly throughout the section.

The base of the Aeronian Stage was defined by the appearance of the *Dem. triangulatus* Biozone graptolite fauna marked by a single occurrence of *Monograptus* (now *Pernerograptus*) austerus sequens (Hutt) in the stratotype section. The highest evidence of the underlying Rhuddanian *C. cyphus* Biozone is provided by an occurrence of *Pernerograptus austerus vulgaris* (Hutt) found 18 m below the boundary "golden spike". Temple (1988) called attention to the faunal distribution in Trefawr track section, as being inadequate to justify selection of the stage boundary stratotype at this section. Moreover, Zalasiewicz *et al.* (2009) noted the restricted stratigraphical range of *Pern. austerus sequens* in the middle part of the *triangulatus* Biozone. Thus, the current base of the Aeronian Stage lies within the *triangulatus* Biozone, and not at the base of the biozone as it is currently used as a tool for global correlation. The nominal index graptolite itself is entirely missing from the stratotype section. In addition, *Pernerograptus austerus sequens* is not an easily

identifiable or common taxon. It has been recorded outside the Britain solely by Bjerreskov (1975) from island of Bornholm, Denmark.

We propose that the FAD of the graptolite *Dem. triangulatus* should be retained as a marker horizon in global correlation of the base Aeronian in order to respect the stability of the stage boundary. The base of the *triangulatus* Biozone has been widely adopted as a marker in global correlation (Zalasiewicz *et al.* 2009; Loydell 2012; Melchin *et al.* 2012, 2020) for this stage. The Silurian was a time of relatively low faunal provincialism among graptolites (Goldman *et al.* 2013), but some differences in graptolite ranges and faunal assemblages between distant areas have been recognised since the preliminary assessment by Melchin (1989). The new stratotype is proposed in an area with strong faunal affinities with the original stratotype area and thus further supports stability of the definition of the Aeronian Stage.

3. Lower Silurian Rhuddanian and Aeronian stages in the Prague Synform

The Palaeozoic succession of the Barrandian area represents the sedimentary cover of the Teplá-Barrandian Unit, which has been considered to be an independent microplate named Perunica (Havlíček *et al.* 1994; Fatka & Mergl 2009), detached from north-western Gondwana, and separate and distant from eastern Cadomian-type terranes (Linnemann *et al.* 2004; Murphy *et. al* 2006). Perunica remained close to Gondwana until the late Silurian (Cocks & Torsvik 2002, 2006, 2013). Another palaeogeographical concept considered the Teplá-Barrandian Unit to be part of the Armorican terrane assemblage or HUN superterrane, which was an integral part of Gondwana until the late Silurian (Stampfli *et al.* 2002; Robardet 2003; von Raumer & Stampfli 2008). The palaeogeographical position of Perunica (and thus of the Teplá-Barrandian Unit) within the Rheic Ocean is uncertain due to its faunal affinities to different palaeocontinents (Ebbestad *et al.* 2013; Eriksson *et al.* 2013; Goldman *et al.* 2013; Kröger 2013; Meidla *et al.* 2013; Molyneux *et al.* 2013) and a wide range of palaeolatitudes have been suggested by palaeomagnetic studies (Tait *et al.* 1994, 1995; Krs & Pruner 1995, 1999; Krs *et al.* 2001; Patočka *et al.* 2003; Aïfa *et al.* 2007; Tasáryová *et al.* 2014).

Silurian rocks are preserved in the Prague Synform – a structure formed during the Variscian Orogeny (Fig. 1) – representing an erosional remnant of a continental rift basin, called the Prague Basin by some authors, infilled by an Ordovician to Middle Devonian marine sedimentary succession with associated basaltic volcanic rocks (for summary see Chlupáč *et al.* 1998).

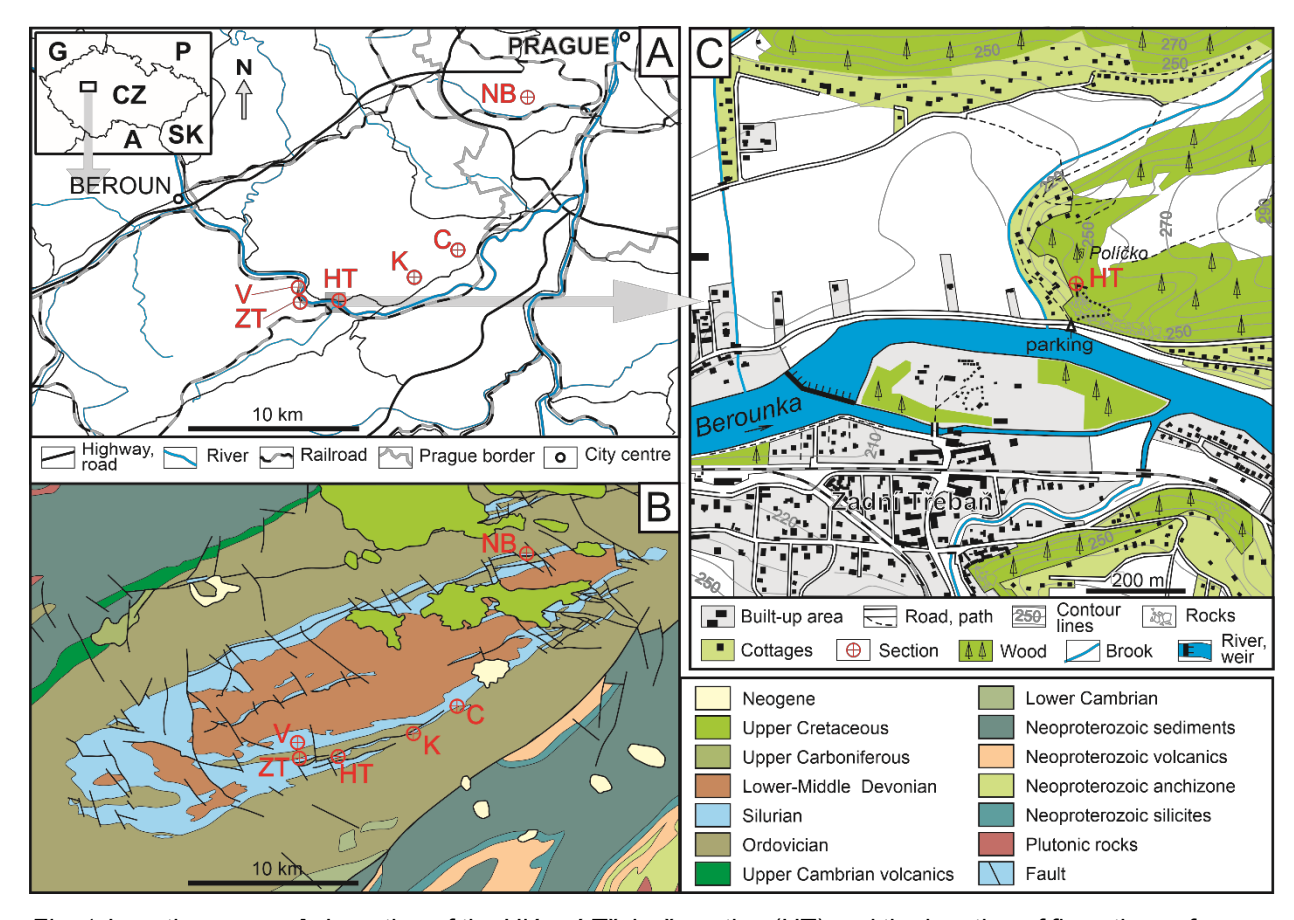


Fig. 1. Location maps: **A**. Location of the Hlásná Třebaň section (HT) and the location of five other reference sections with the Rhuddanian-Aeronian boundary strata; Karlík (K), Černošice (C), Zadní Třebaň (ZT), Vočkov (V), and Nové Butovice (NB). Small inset shows generalized location of the study area in central Europe (CZ – Czech Republic, SK – Slovakia, G – Germany, A – Austria, P – Poland). **B**. Simplyfied geological map of the Prague Synform showing the same territory and sections as map A. **C**. Detailed location of the Hlásná Třebaň section. After Štorch *et al.* (2018).

In the Prague Synform, both the Rhuddanian and Aeronian stages are represented by the Želkovice Formation comprising an 8–12 m thick, condensed off-shore marine, anoxic sedimentary succession (Kříž 1998). Black silty shales, siliceous shales and thin-bedded silicites predominate, and clayey shales are confined to the lowermost part of the Želkovice Formation (Štorch 2006). Strata are rich in graptolites (Bouček 1953; Štorch 1994, 2023) associated with organic walled microfossils (Dufka *et al.* 1995). Graptolites, in particular, have been used as an effective tool for long-range correlation with high precision. Shelly faunas are very rare.

The Želkovice Formation overlies the pale-coloured uppermost Hirnantian mudstones of the Kosov Formation. The onset of the anoxic black shale sedimentation coincided almost precisely with the base of the lowermost Silurian *Akidograptus ascensus* Biozone (Horný 1956; Štorch 1986). Sedimentation temporarily ceased in the early Rhuddanian, revived in the upper part of the *Cystograptus vesiculosus* Biozone in the majority of studied sections (Fig. 2) of the Prague Synform, and continued without interruption across the Rhuddanian-Aeronian boundary interval

and through the entire Aeronian until deposition of a non-fossiliferous beds of pale-coloured mudstone and claystone marking the base of the succeeding Litohlavy Formation of Telychian age (Kříž 1975; Štorch 2006; Štorch & Frýda 2012). The most complete black-shale succession, with little or no gap in sedimentation, is developed in the southwestern and northeasternmost parts of the Prague Synform including the Hlásná Třebaň section. In many sections the lower Silurian black-shale succession is disrupted by alkaline doleritic basalt sills (Kříž 1998). The subsequent Variscan Orogeny affected the Želkovice Formation only slightly, as demonstrated by only minor and local folding, subordinate faulting, and low to moderate thermal maturity (Kříž 1998).

4. Rhuddanian-Aeronian boundary sections of the Prague Synform

Based on earlier stratigraphical studies devoted to the Llandovery strata of the Barrandian area and their correlation with other European regions (Bouček 1953; Štorch 1986, 2006), six localities qualified for closer examination of the Rhuddanian-Aeronian boundary strata (Štorch *et al.* 2018): Hlásná Třebaň (49°55′22,93″ N, 14°12′42,97″E), Karlík (49°56′30,02″N, 14°16′8,58″E), Vočkov (49°55′34,10″N, 14°10′53,60″E), Zadní Třebaň (49°55′10,48″N, 14°11′5,80″E), Černošice (49°57′27,06″N, 14°18′22,98″E) and Nové Butovice (50°2′51,11″N, 14°20′37,53″E) (Figs 1, 2). All sections exhibit similar sedimentary successions across the Rhuddanian-Aeronian boundary. Minor differences were found in thickness, facies details and stratigraphical extent of disconformities. The graptolite succession is almost identical in all of the sections, minor differences are the result of preservational artefacts and sampling biases coupled with variations in lithology, weathering, and the thermal effects of neighbouring basalt sills.

5. The Hlásná Třebaň section

Of the sections listed above, the Hlásná Třebaň section (Figs. 2, 3, 4), exposed on the hillside high above the road from Hlásná Třebaň to Lety (Fig. 3A) on the left (north) bank of Berounka River, exhibits the most complete, most readily accessible and least thermally and tectonically affected Rhuddanian—Aeronian sedimentary succession with continuous and lithologically monotonous sedimentation across the broad boundary interval. The section has yielded abundant, diverse and usually well-preserved graptolites, identifiable chitinozoans, and a clear carbon and nitrogen isotope record. The locality was first briefly described by Kodym *et al.* (1931) and Přibyl (1937). A more detailed description and full list of references were provided by Kříž (1992), including a preliminary log and graptolite range chart of the Rhuddanian and Aeronian strata based upon the

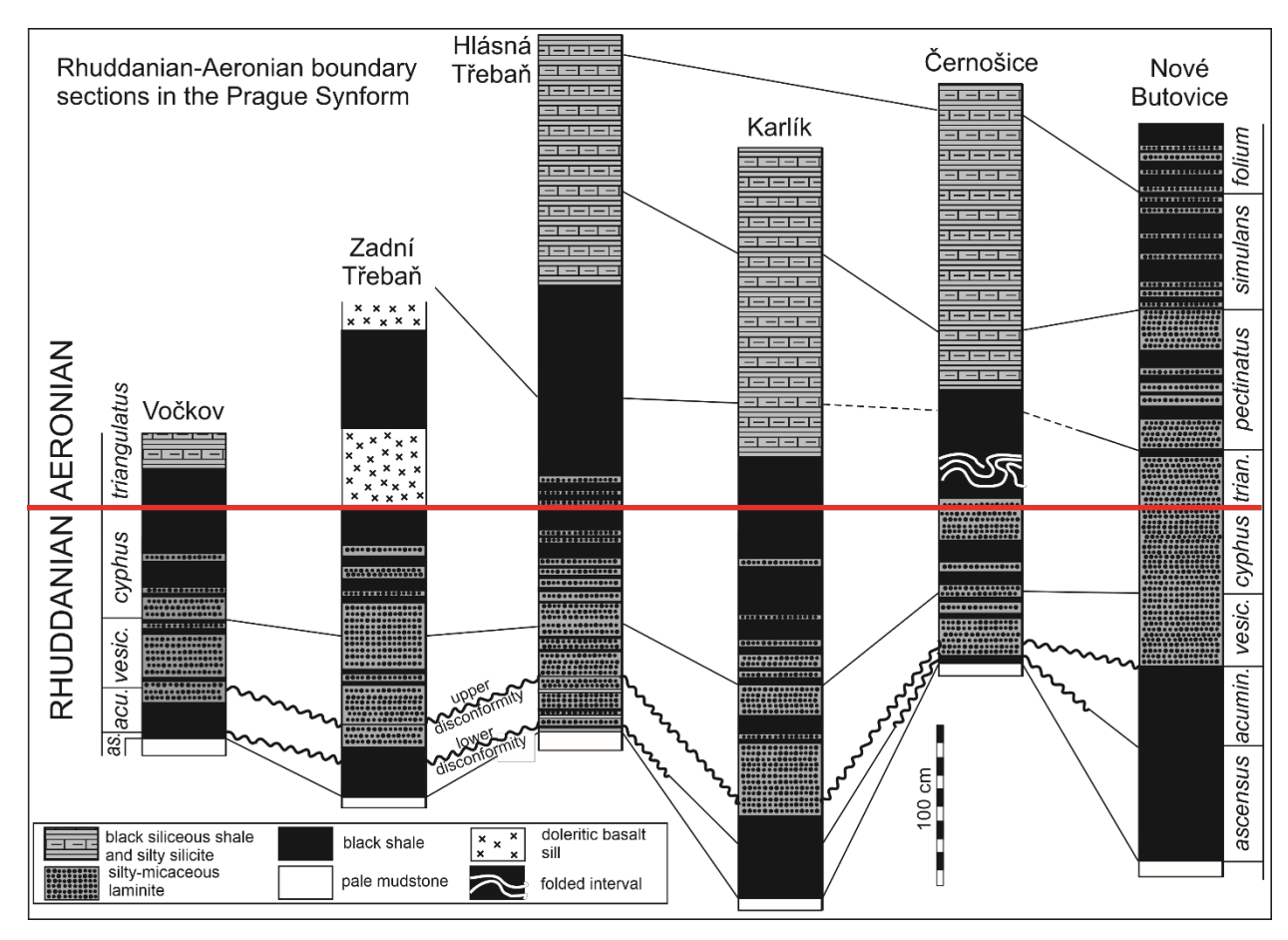


Fig. 2. Correlation of Rhuddanian-Aeronian sections exposed in the southern limb and north-eastern limb of the Prague Synform. Simplified section logs after Štorch et al. (2018), updated. Abbreviations: as. – ascensus Biozone, acu., acumin. – acuminatus Biozone, vesic. – vesiculosus Biozone, trian. – triangulatus Biozone. After Štorch et al. (2018), updated.

unpublished thesis of Štorch (1991). Štorch (2006) published a generalized sedimentary log also including the Hirnantian sequence. Chitinozoan and acritarch data from the uppermost Hirnantian and Rhuddanian strata were discussed by Dufka & Fatka (1993). Frýda & Štorch (2014) published the first data on the C_{org} isotope record and TOC from the Hlásná Třebáň section covering the stratigraphic interval from the Ordovician-Silurian boundary to the *convolutus* Biozone. A detailed description of the section and evaluation of its correlative potential were published by Štorch *et al.* (2018).

The section begins with the Hirnantian sedimentary succession exposed above a massive sill of Silurian doleritic basalt and starts with silty shales of the middle part of the Kosov Formation. In the middle of the hill slope, marine storm-dominated sandstones of the upper Kosov Formation rest on this shaly succession with a prominent erosional disconformity (Brenchley & Štorch 1989; Štorch 2006). Several pulses of clast-supported conglomerates with sandstone matrix infilled a shallow channel incised unconformably into the soft shale. The conglomerates are overlain by packets of coarse, upward-fining sandstone beds with rip-up clasts, internal erosion



Fig. 3. Hlásná Třebaň Section – field photographs: A. Rhuddanian and lower Aeronian black shales outcropping downslope of the sampled exposure. Red bar indicates the base of the Aeronian Stage. B. Sampled section after first round of sampling. Red line marks base of the *triangulatus* graptolite Biozone and proposed Rhuddanian-Aeronian boundary. C. Rhuddanian-Aeronian boundary beds in detail. After Štorch *et al.* (2018).





surfaces and hummocky cross-stratification. Wave ripples and hummocky cross-stratification are also developed in succeeding couplets of fine-grained sandstones and silty micaceous shale. The upward-fining sequence near the top of the Kosov Formation reflects the late Himantian post-glacial rise in sea-level (Brenchley & Štorch 1989; Štorch 2006).

The Ordovician-Silurian boundary is exposed a few metres below the upper hill-slope edge. It is marked by an abrupt change from the yellowish bioturbated clay mudstone of the topmost Kosov Formation to black shales of the lowermost Želkovice Formation, with graptolites of the basal Silurian *Akidograptus ascensus* Biozone. Rhuddanian sedimentation, dominated by graptolite-rich black silty-micaceous laminites was interrupted by two discrete disconformities (Figs. 2, 4). The upper *A. ascensus* and/or lowermost *Parakidograptus acuminatus* biozones are

missing at the lower disconformity, and the upper *Par. acuminatus* and lower *Cystograptus vesiculosus* biozones are missing at the upper disconformity. An uninterrupted black shale succession begins with the upper *Cystograptus vesiculosus* Biozone and continues through the *Coronograptus cyphus* Biozone, across the Rhuddanian-Aeronian boundary, and then through the *Demirastrites triangulatus* Biozone, *Demirastrites pectinatus* Biozone, *Demirastrites simulans* Biozone and *Pribylograptus leptotheca* Biozone, up to the middle Aeronian *Lituigraptus convolutus* Biozone, which is slightly thermally altered by an overlying basalt sill.

5a. Fossil record and biostratigraphy

Particular attention was focused on the rich, high-diversity graptolite assemblages preserved on each bedding plane in the Rhuddanian and Aeronian black-shale succession of the Želkovice Formation at Hlásná Třebaň. Each 10 cm thick interval of the section was sampled in two rounds and every graptolite, at least considered to be tentatively identifiable, was collected from a rock volume of c. 0.03 m³ per sample. Higher resolution sampling intervals, 5 cm thick, were used within the immediate interval of the Rhuddanian-Aeronian boundary strata. The graptolite collections comprised about 5000 specimens of 65 species determined from the *Akidograptus ascensus*—lowermost *Demirastrites simulans* biozones. 59 species were identified by Štorch *et al.* (2018) and Štorch & Melchin (2018), in the upper *vesiculosus*—lowermost *simulans* biozones. The graptolite material is housed in the Czech Geological Survey, Prague, in the collection prefixed with PŠ. A full list of graptolites and their stratigraphic ranges from the upper *vesiculosus* to the lower *simulans* biozones are shown in Fig. 4.

The Silurian succession (Fig. 4) begins with the fine black shale of the lowermost Želkovice Formation with graptolites of the basal Silurian ascensus Biozone, in particular Neodiplograptus lanceolatus Štorch & Serpagli, and A. ascensus Davies. The lowermost, less than 5 cm thick, clayey black shale is separated by a discrete disconformity from overlying black silty-micaceous laminites (Fig. 4) with graptolites of the middle acuminatus Biozone: Par. acuminatus (Nicholson), A. ascensus, Neodiplograptus apographon (Štorch), Nd. lanceolatus, Cystograptus ancestralis Štorch, Normalograptus longifilis (Manck) and Normalograptus cf. ajjeri (Legrand). This assemblage was discussed in a broader biostratigraphical and palaeobiogeographical context by Štorch (1996) and the species present are not listed in the range chart on Figure 4. The well-preserved graptolites are confined to a fine black shale interval associated with a 2 cm thick grey mudstone without graptolites, 22 cm above the base of the black shale succession.

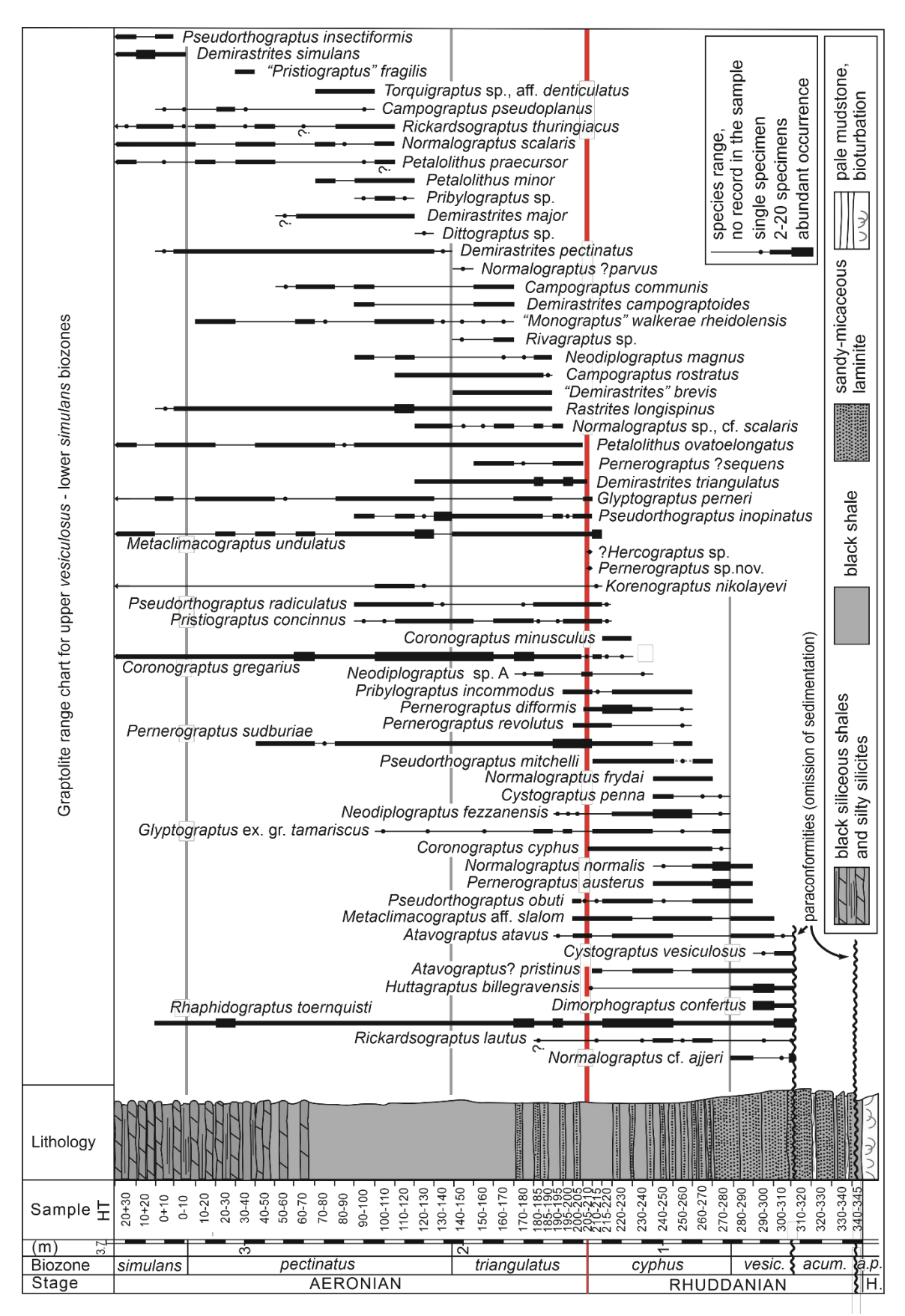


Fig. 4. Stratigraphy, lithology, sampling intervals and graptolite range-chart of the Rhuddanian-Aeronian Hlásná Třebaň section. Base of the Aeronian Stage marked by red line. Abbreviations: vesic. – vesiculosus Biozone, acum. – acuminatus Biozone, a. – ascensus Biozone, p. – supposed Metabolograptus persculptus Biozone, H – Hirnantian. After Štorch et al. (2018), updated.

The upper acuminatus and lower vesiculosus biozones are missing due to another gap in sedimentation developed across the basin. The latter disconformity separates the middle acuminatus Biozone from silty-micaceous laminites crowded with unfavourably preserved graptolites indicating the upper part of the vesiculosus Biozone. Dimorphograptus confertus (Nicholson), Rhaphidograptus toernquisti (Elles & Wood), Huttagraptus billegravensis Koren' & Bjerreskov, Atavograptus atavus (Jones), Atavograptus? pristinus (Hutt) and the minute Metaclimacograptus aff. slalom (Zalasiewicz) have been recognized in this 33 cm thick interval along with the biozonal index Cystograptus vesiculosus (Nicholson) and some poorly preserved and difficult to identify normalograptids and metaclimacograptids.

The Coronograptus cyphus Biozone comprises 0.73 m thickness of silty-micaceous laminites passing upward into thin-bedded shale with subordinate silty-micaceous laminas. This biozone represents an interval between the lowest occurrence of C. cyphus (Lapworth) and lowest occurrence of Demirastrites triangulatus (Harkness). The latter almost precisely coincides with the highest occurrence of C. cyphus. The latter taxon (Fig. 5S, T) is moderately common through the whole thickness of the cyphus Biozone. The graptolite assemblage also includes the robust Neodiplograptus fezzanensis (Desio) (Fig. 5J) and Pseudorthograptus obuti (Rickards & Koren') (Fig. 5G, Q), associated with Normalograptus frydai Storch (Fig. 5B), Cystograptus penna (Hopkinson) (Fig. 5C, E), Pseudorthograptus mitchelli Štorch (Fig. 5O), Glyptograptus ex gr. tamariscus, abundant Rhaphidograptus toernquisti (Fig. 5D), Pribylograptus incommodus (Törnquist) (Fig. 5A), Pernerograptus sudburiae (Hutt) (Fig. 5H) and Pernerograptus austerus (Törnquist). Coronograptus gregarius (Lapworth), rare Coronograptus minusculus Obut & Sobolevskaya (Fig. 5M), uncommon Pernerograptus revolutus (Kurck) (Fig. 5I) and abundant Pernerograptus difformis (Törnquist) (Fig. 5L,R) occur in the upper part of this biozone along with several other taxa (see Fig. 4). The uppermost two 5 cm thick sampling levels of the *cyphus* Biozone yielded the lowest occurrences of Pristiograptus concinnus (Lapworth), Metaclimacograptus undulatus (Kurck) and Pseudorthograptus radiculatus (Manck) (Fig. 5F) identified as Pseudorthograptus finneyi by Štorch et al. (2018). Pseudorthograptus inopinatus (Bouček) and Glyptograptus perneri Štorch appear only a few centimetres below the FAD of Demirastrites triangulatus (Harkness). Also a single specimen of Pernerograptus sp. nov., an easily recognizable species (Fig. 5K), confined to the uppermost cyphus Biozone in Spain (PŠ, personal observation), came from this level.

Fine black shales with abundant and well-preserved graptolites (Fig. 6) occur across the Rhuddanian-Aeronian boundary interval. The base of the Aeronian Stage is here considered to coincide with the base of the *Demirastrites triangulatus* Biozone, defined by the lowest and

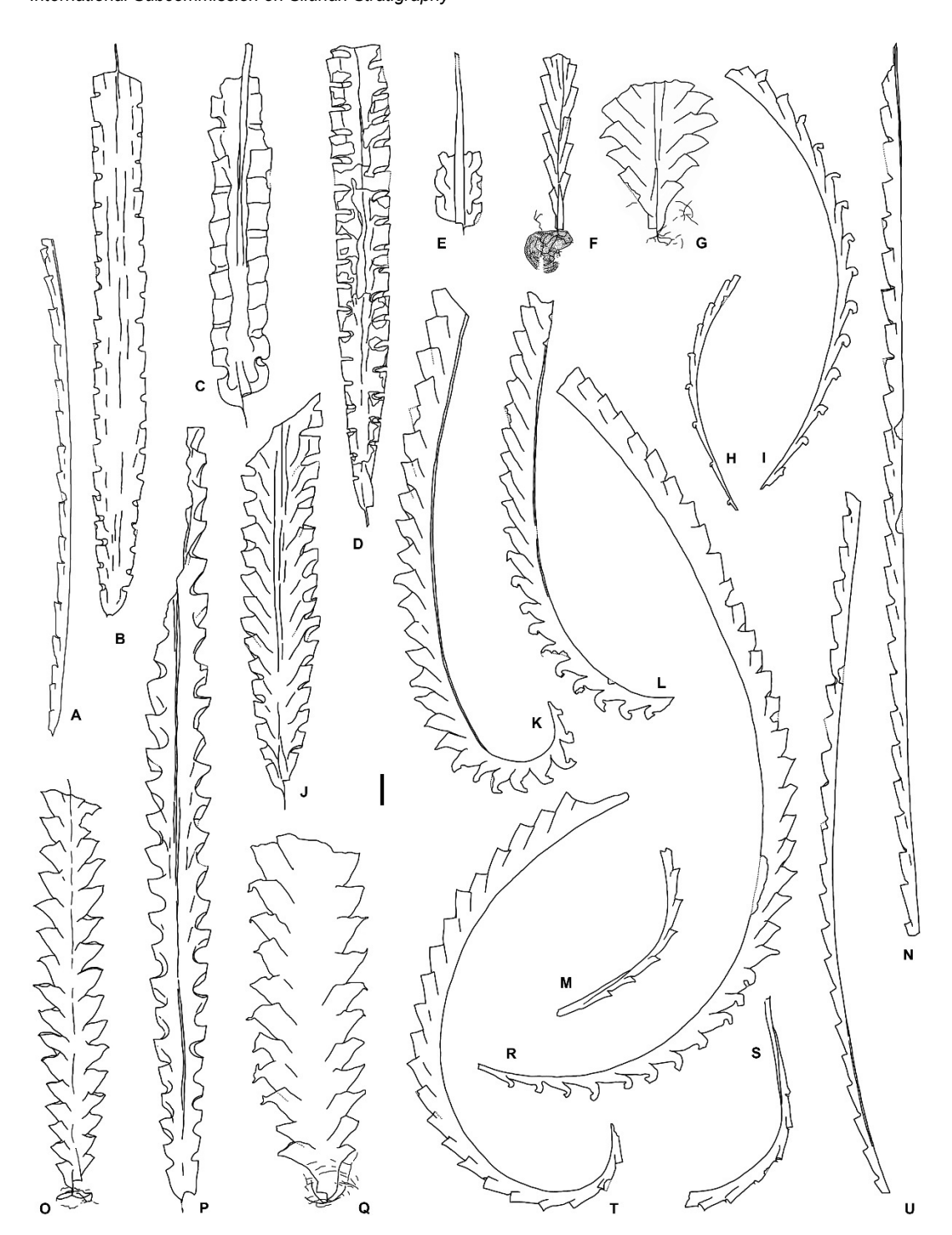


Fig. 5. Graptolite fauna of the upper Rhuddanian Coronograptus cyphus Biozone — selected taxa. A. Pribylograptus incommodus (Törnquist), PŠ4083, mesial fragment from HT207-210. B. Normalograptus frydai Štorch, PŠ3563 from the lower part of the Biozone. C. E. Cystograptus penna (Hopkinson), C. PŠ3428, middle part of the Biozone. E. PŠ3964, juvenile rhabdosome from HT240-250. D. Rhaphidograptus toernquisti (Elles &Wood), PŠ 3964, HT240-250. F. Pseudorthograptus radiculatus (Manck), PŠ3945, HT205-210. G. Q. Pseudorthograptus obuti (Rickards & Koren'), G. PŠ4142, HT207-210, Q. PŠ3462, upper part of the Biozone. H. Pernerograptus sudburiae (Hutt), PŠ4006, mesial fragment from HT220-230. I. Pernerograptus revolutus (Kurck), PŠ3914, mesial fragment from HT210-215. J. Neodiplograptus fezzanensis (Desio), PŠ4013/3, HT240-250. K. Pernerograptus sp. nov., PŠ3965, HT207-210. L. R. Pernerograptus difformis (Törnquist); L. PŠ4280, mesial part from the uppermost cyphus Biozone, R. PŠ3961, HT207-210. M. Coronograptus minusculus Obut & Sobolevskaya, PŠ3919, HT207-210. N. U. Atavograptus atavus (Jones); N. PŠ4088, distal fragment from HT207-210, U. PŠ4109, sub-proximal part from HT220-230. O. Pseudorthograptus mitchelli Štorch, PŠ3915, HT220-230. P. Korenograptus nikolayevi (Obut), PŠ3953, HT210-215. S. T. Coronograptus cyphus (Lapworth); S. PŠ4279/2, proximal part from the middle cyphus Biozone, T. PŠ3950, HT210-215. A, D–K, M–P, R, T, U from the Hlásná Třebaň Section (HT); B, C, L, Q, S from Všeradice described by Štorch (2015). Scale bar represents 1 mm. After Štorch et al. (2018), updated.

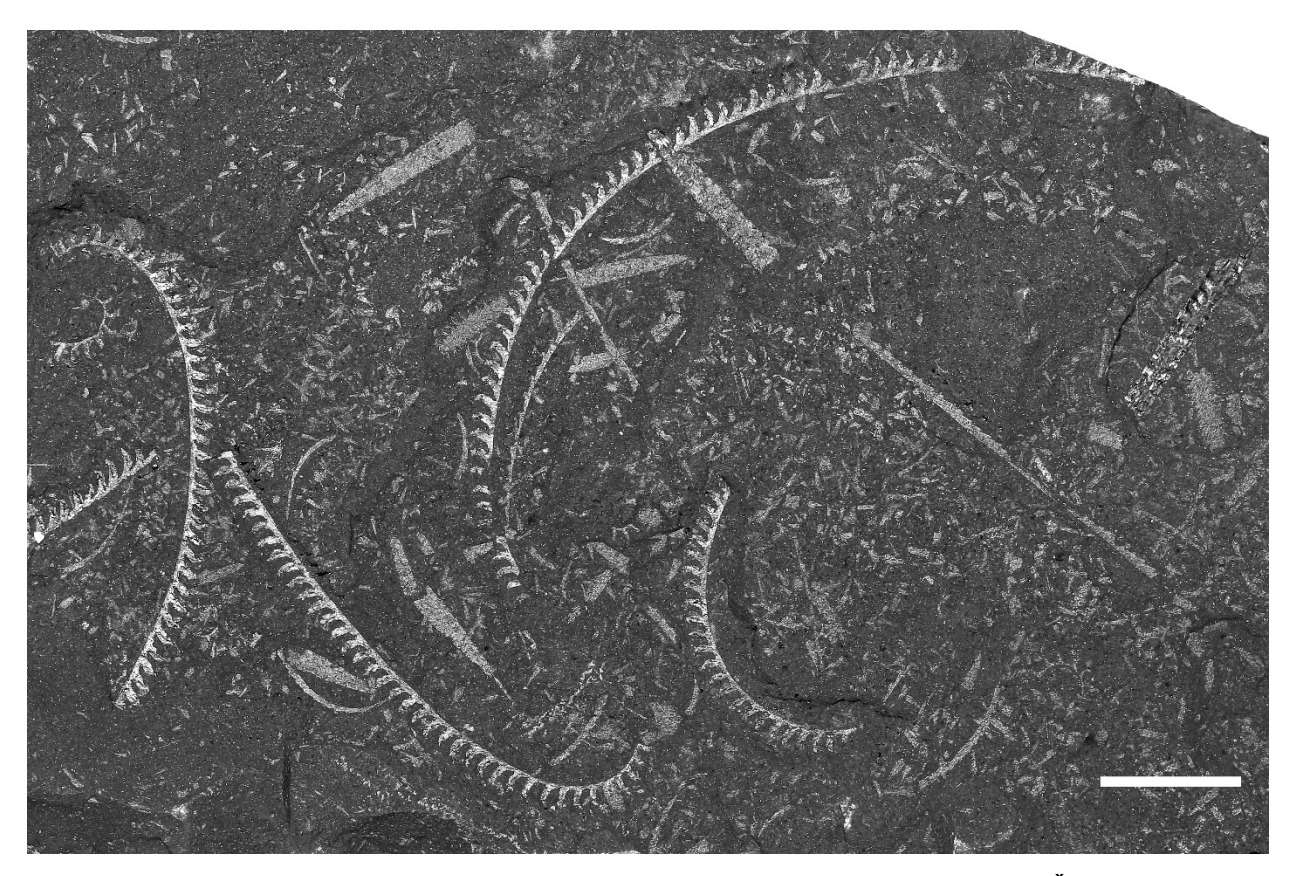


Fig. 6. Slab from the lower part of the *triangulatus* Biozone at Hlásná Třebaň Section (PŠ4281, Sample HT 190-195) showing graptolite assemblage dominated by the zonal index fossil *Demirastrites triangulatus* (Harkness). Scale bar represents 10 mm.

immediately abundant occurrence of the eponymous graptolite, *Dem. triangulatus* (Fig. 7L–N) [= *Monograptus separatus triangulatus* of Sudbury (1958)] 1.38 m above prominent and abrupt change in lithology from pale colored, yellowish mudstones of the topmost Kosov Formation to black graptolitic shales of the Želkovice Formation (see Fig. 4). The lowermost part of the 0.67 m thick *Dem. triangulatus* Biozone is marked by a rapid graptolite diversification, including the successive appearances of several new lineages, mostly of monograptids with isolated and hooked thecae (first *Demirastrites*, then *Rastrites* and *Campograptus*) as well as the first species of *Petalolithus* with its tabular, biserial rhabdosome. *Petalolithus ovatoelongatus* (Kurck) (Fig. 7Q) appeared in the first 5 cm thick sample above the boundary stratum. Also, *Rastrites longispinus* Perner (Fig. 7G, H), *Campograptus rostratus* (Elles & Wood) (Fig. 7P), *Demirastrites brevis* (Sudbury) (7D), and, surprisingly, the robust *Neodiplograptus magnus* (Lapworth) (7I) joined the assemblage in the lower part of the *triangulatus* Biozone, whereas *Campograptus communis* (Lapworth), *Demirastrites campograptoides* Štorch & Melchin (Fig. 7J) and "*Monograptus*" *walkerae rheidolensis* Rickards, Hutt & Berry appeared in the upper part of the biozone. In turn, *Atavograptus*? *pristinus* and *C. cyphus* disappeared at the top of the *cyphus* Biozone and the last

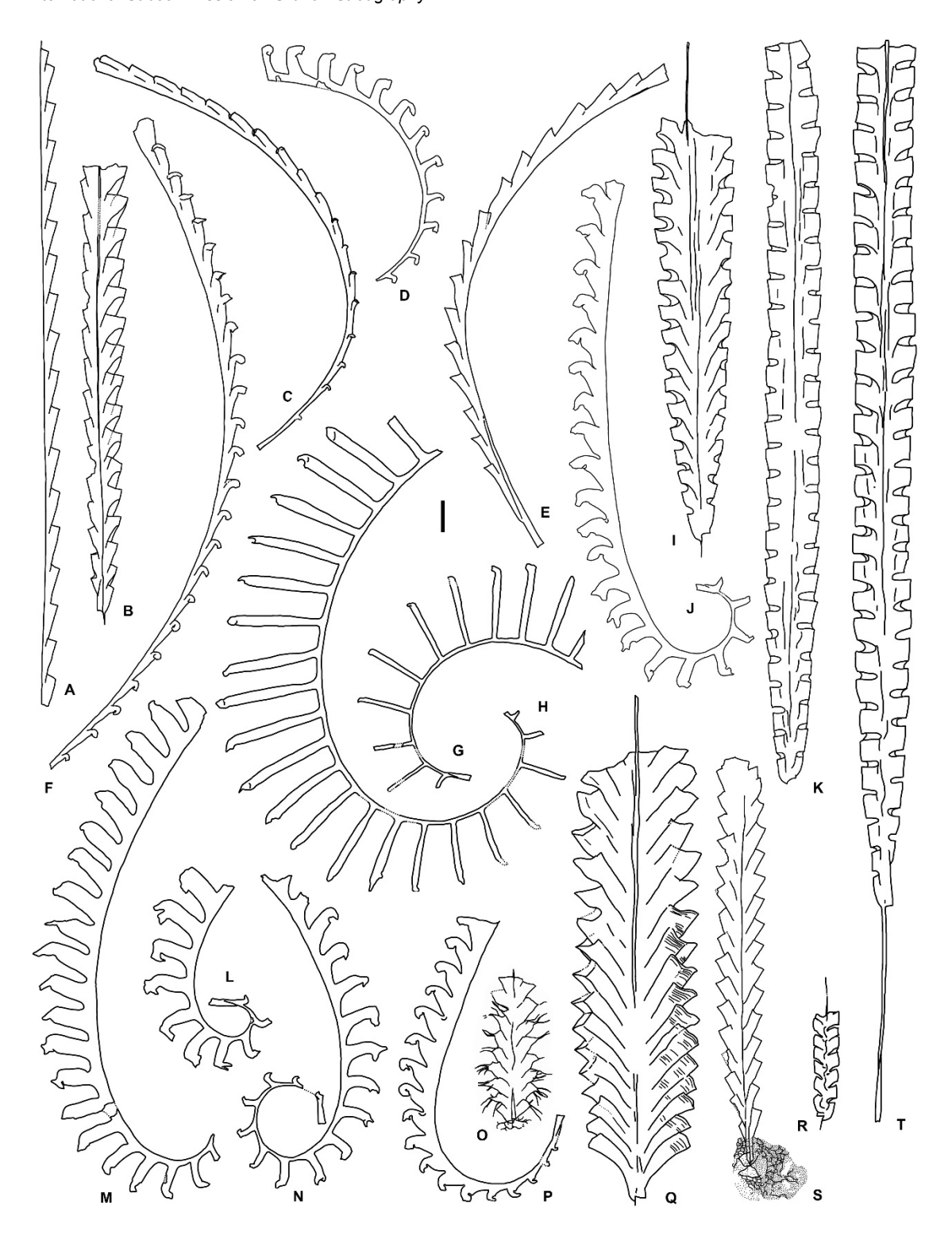


Fig. 7. Graptolite fauna of the lowermost Aeronian Demirastrites triangulatus Biozone — selected taxa. A. Pristiograptus concinnus (Lapworth), PŠ3949, mesial part from HT180-190. B. Glyptograptus perneri Štorch, PŠ3943, HT205-207. C. Pernerograptus sudburiae (Hutt), PŠ3910b, HT200-205. D. Demirastrites? brevis (Sudbury), PŠ4162, HT180-185. E. Coronograptus gregarius (Lapworth), PŠ 3922, HT150-160. F. Pernerograptus revolutus (Kurck), PŠ3959, HT205-207. G. H. Rastrites longispinus Perner; G. PŠ4103a, HT140-150, H. PŠ3954, HT160-170. I. Neodiplograptus magnus (H. Lapworth), PŠ3916, HT180-190. J. Demirastrites campograptoides Štorch & Melchin, PŠ3988a, HT160-170. K. Normalograptus sp., cf. scalaris (Hisinger), PŠ 3956, HT185-190. L–N. Demirastrites triangulatus (Harkness); L. PŠ4219, HT195-200, M. PŠ4220, HT195-200, N. PŠ4224 early morphotype common in HT200-205. O. Pseudorthograptus inopinatus (Bouček), PŠ3923, HT205-207. P. Campograptus rostratus (Elles & Wood), PŠ3912, HT140-150. Q. Petalolithus ovatoelongatus (Kurck), HT160-170. R. Metaclimacograptus undulatus (Kurck), PŠ4131, HT180-185. S. Pseudorthograptus radiculatus (Manck), PŠ3948, HT205-207. T. Rhaphidograptus toernquisti (Elles &Wood), PŠ4150, HT160-170. All specimens from the Hlásná Třebaň Section, scale bar represents 1 mm. After Štorch et al. (2018), updated.

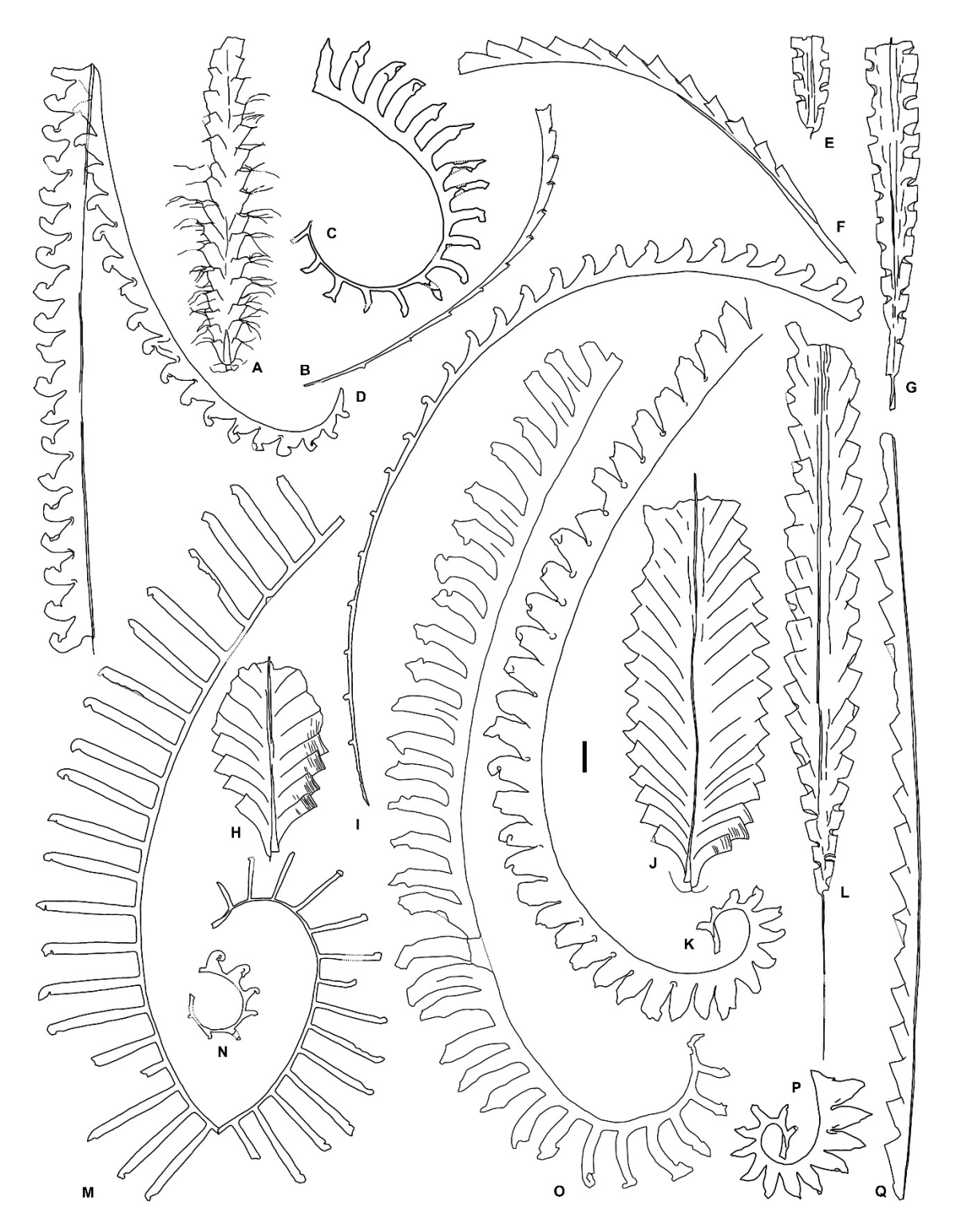


Fig. 8. Graptolite fauna of the lower Aeronian Demirastrites pectinatus Biozone — selected taxa. A. Pseudorthograptus inopinatus (Bouček), PŠ4011, HT120-130. B. Pernerograptus? chrysalis (Zalasiewicz), PŠ4020, mesial part from HT120-130. C. O. Demirastrites major (Elles & Wood); C. PŠ3925, HT90-100, O. PŠ 3929, HT90-100. D. Campograptus communis (Lapworth), PŠ3960, broken rhabdosome from HT120-130. E. Normalograptus scalaris (Hisinger), PŠ4102, juvenile rhabdosome from HT40-50. F. Coronograptus gregarius (Lapworth), PŠ3918, late form with long sicula from HT90-100. G. Rhaphidograptus toernquisti (Elles &Wood), PŠ4106/2, HT30-40. H. Petalolithus minor (Elles), PŠ3951, HT70-80. I. "Monograptus" walkerae rheidolensis Rickards et al., PŠ4009, HT100-110. J. Petalolithus ovatoelongatus (Kurck), PŠ4018, HT90-100. K, P. Demirastrites pectinatus (Richter); K. PŠ4057, HT70-80, P. PŠ3931, HT90-100. L. Rickardsograptus thuringiacus (Kirste), PŠ4100, HT10-20. M. Rastrites longispinus Perner, PŠ4015, broken mature rhabdosome from HT110-120. N. Torquigraptus sp. aff. denticulatus (Törnquist), PŠ4068a, juvenile specimen from HT70-80. Q. Pristiograptus concinnus (Lapworth), PŠ4125, mesial fragment from HT130-140. All specimens from the Hlásná Třebaň Section, scale bar represents 1 mm. After Štorch et al. (2018).

Ps. obuti was found a few centimetres above the biozonal boundary at the level where Pet. ovatoelongatus made its lowest occurrence. Nd. fezzanensis, At. atavus (Fig. 5N, U), Pern. revolutus, Pern. difformis and Prib. incommodus have their highest occurrences in the lower part of the triangulatus Biozone. In total, 31 graptolite species have been found in the triangulatus Biozone of the Hlásná Třebaň section.

The diversification of triangulate monograptids continued (Štorch & Melchin 2018) through the succeeding, 1.34 m thick *Demirastrites pectinatus* Biozone. Along with the proliferation of C. gregarius (Fig. 8F) and R. longispinus (Fig. 8M), demirastritids further diversified, being represented by the biozonal index *Demirastrites pectinatus* (Richter) (Fig. 8K, P) [= M. fimbriatus (Nicholson)] and *Demirastrites major* (Elles & Wood) (8C, O) with its long, ventrally curved thecae and an elongated proximal part. Dem. triangulatus last appeared in the lower part of the pectinatus Biozone along with Pr. concinnus (Fig. 8Q), Ps. radiculatus and the previously fairly common Ps. inopinatus (Fig. 8A). The Campograptus lineage gave rise to Campograptus pseudoplanus (Sudbury) with an elongated proximal part. Uncommon "Monograptus" walkerae rheidolensis (Fig. 8I) continued to the upper part of the biozone. Pernerograptus with its biform thecae isrepresented by Pern. sudburiae and less common Pern. chrysalis (Zalasiewicz) (Fig. 8B). Pribylograptus sp. with long ventral apertural spines closely resembles the species figured by Loydell et al. (2003) from the triangulatus Biozone of Latvia. Rh. toernquisti (Fig. 8G) dominated among the biserial and unibiserial taxa, being accompanied by Metacl. undulatus, Gl. perneri, Normalograptus scalaris (Hisinger) (Fig. 8E), Rickardsograptus thuringiacus (Kirste) (Fig. 8L), Petalolithus minor (Elles) (Fig. 8H), Pet. ovatoelongatus (Fig. 8J), and the lowest specimens of Petalolithus praecursor Bouček & Přibyl. Robust rhabdosomes of Nd. magnus, spinose Ps. inopinatus and wedge-shaped Ps. radiculatus have their highest occurrences in the lower and/or middle part of the pectinatus Biozone the total graptolite fauna comprises 30 species. Black shales are gradually replaced by siliceous strata in the upper part of the pectinatus Biozone, including silty silicites that alternate with siliceous shales through the succeeding 1 m thick Demirastrites simulans Biozone. Dem. simulans (Pedersen) and Pseudorthograptus insectiformis (Nicholson), are associated with taxa continuing from the lower part of the *pectinatus* Biozone, whereas *Dem*. pectinatus, R. longispinus and Rh. toernquisti vanish from the fossil record. Higher up, beyond the succession presented on Figure 4, Rastrites geinitzii Törnquist, Monograptus mirus Perner and Campograptus millepeda (McCoy) joined the assemblage of the simulans Biozone in the Hlásná Třebaň section.

Black siliceous shales interbedded with platy, black silty silicites compose the 1.3 m thick *Pribylograptus leptotheca* Biozone and the more than 2 m thick lower half of the *Lituigraptus convolutus* Biozone. The latter biozone is thermally altered by an overlying *ca* 2 m thick basalt sill that intruded the overlying black shales and pale-coloured mudstones of the lower Lithohlavy Formation. Graptolites are less well preserved and difficult to collect from the thermally affected silicites but the general faunal composition matches that described by Štorch (1998) from Tmaň.

The section was also sampled for organic walled microfossils using the same regular intervals (10 cm and 5 cm) from the Silurian-Ordovician boundary to base of *simulans* Biozone. 42 samples were analyzed by Butcher (2016) and Vodička & Butcher (2023).

The obtained chitinozoans show a relatively diverse assemblage that includes typical lower Silurian genera, such as *Angochitina*, *Ancyrochitina*, *Belonechitina*, *Conochitina*, *Cyathochitina*, *Sphaerochitina* and *Spinachitina*. However, the preservation of chitinozoans varies from moderate to poor and hampers exact determination of some species. Preliminary analyses conducted by Butcher (2016) complement and extend through the lower Aeronian earlier, largely Rhuddanian chitinozoan data published by Dufka & Fatka (1993). Data from Butcher (2016), Vodička & Butcher (2023), and Fig. 9 indicate that boundary interval occurs within the *Spinachitina maennili* chitinozoan Biozone, which is consistent with data from the type Llandovery area (Davies *et al.* 2013).

Spinachitina cf. maennili reported from the Hlásná Třebaň section represents a taxon morphologically similar to S. maennili (Nestor, 1980). The taxon has been left in open nomenclature here, however, due to some differences in morphology, dimensions and the absence of preserved spines in the Hlásná Třebaň specimens in comparison to the type material. The difficulties of confident identification due to poor preservation of this taxon were noted also by De Weirdt et al. (2019, p. 18), who stated that it is difficult to differentiate between Conochitina electa (the eponymous species of the underlying C. electa Biozone) and damaged specimens of S. maennili. The Spinachitina maennili biozone has been established as a global biozone ranging the interval of the uppermost Rhudannian to the lower Aeronian (Verniers et al. 1995). However, the species has been reported only in the tropical realm so far, i.e. Baltica (Nestor 1980, 1994, 1999; Grahn 1988, 1995; Loydell et al. 2010 and Männik et al. 2015), Laurentia (Grahn 1985) and Avalonia (Davies et al. 2013; De Weirdt et al. 2019). Although Verniers et al. (1995) referred to Paris et al. (1995) for the occurrence of S. maennili in Saudi Arabia, Paris et al. (2015) later included these specimens in the synonymy of S. geerti Paris, 2015. Thus the applicability of S. maennili Biozone as a global zone is called into question, as an unequivocal report of S. maennili outside the tropical realm is still missing. Nestor (1994, p. 123 and Nestor 1998, p. 226) also

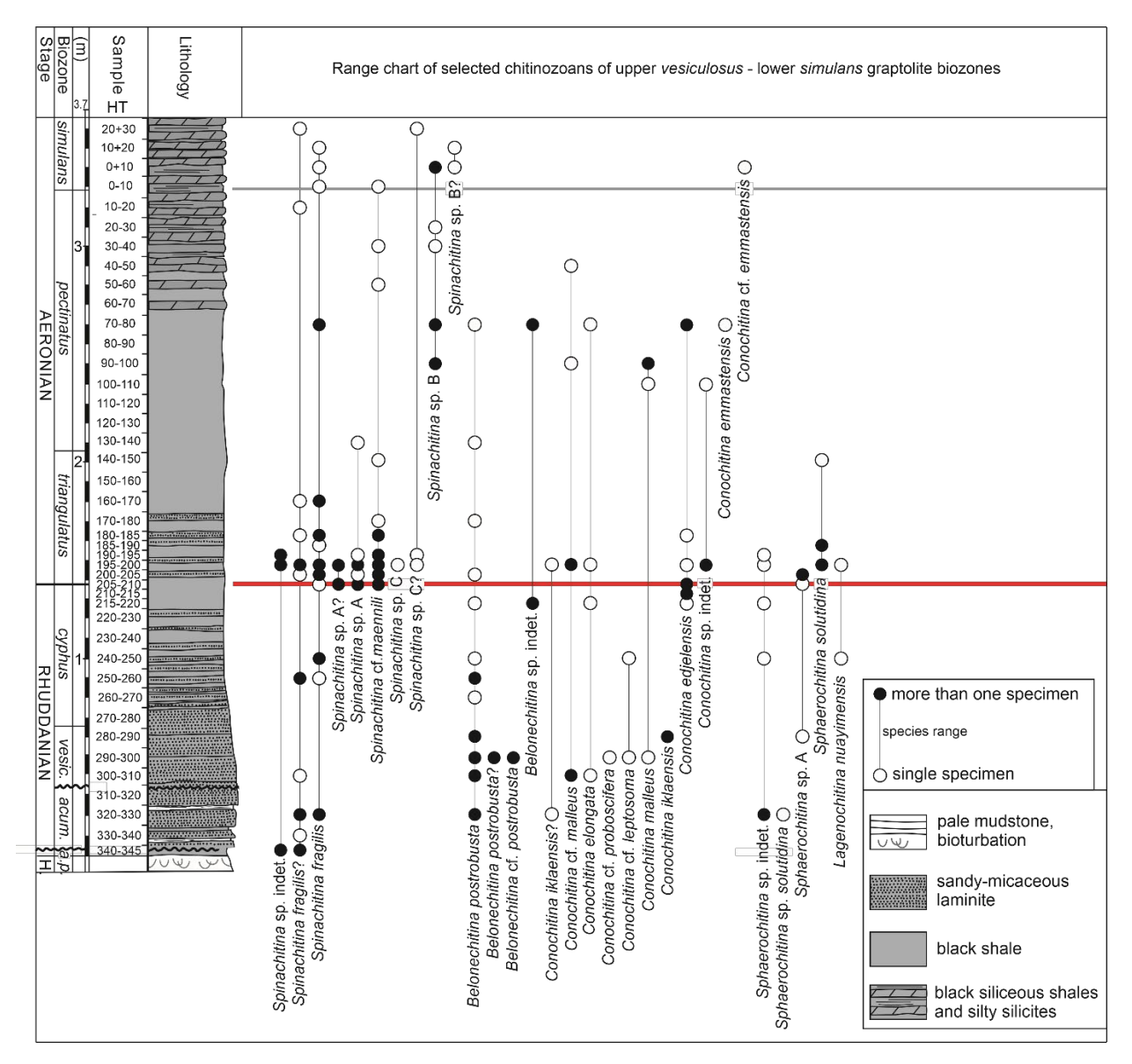


Fig. 9. Range chart of selected chitinozoans from upper *vesiculosus*—lower *simulans* graptolite biozones of the Hlásná Třebaň section.

reported that *S. maennili* occurs 'in deeper-water sections', and the absence of this index taxon in shallow water is further discussed by Nestor (1998) and Loydell *et al.* (2010).

In the Hlásná Třebaň section, *S.* cf. *maennili* appears in in the same level as *D. triangulatus*, i.e. the FAD of *S.* cf. *maennili* is coincident with the proposed base of Aeronian (Fig. 9). The same level is marked by the appearance of another species, *Spinachitina* sp. A. However, *S.* sp. A represents a new species and its correlation potential is thus limited. Other chitinozoan species are either long ranging or have a limited abundance and do not show much correlation potential. What is clear, however, is that the Rhuddanian-Aeronia boundary in the section herein sees a significant appearance of new taxa at or just above the boundary horizon. However, due to poor preservation and the uncertainties regarding the taxa within the genus *Spinachitina* (which is recognised by

most chitinozoan authors as being in need of detailed revision), these are retained largely in open nomenclature and cannot yet be correlated globally with confidence. Echoing the statement of De Weirdt *et al.* (2019) for the proposed Rheidol Gorge GSSP section therein, the chitinozoans in the Hlásná Třebaň section may 'act as an auxiliary marker for the boundary level, albeit not a very precise one'.

5b. Sedimentary succession

Three principal hemipelagic lithotypes (Fig. 10) are developed in the lower Silurian Želkovice Formation in the Hlásná Třebaň section. The stratigraphical distribution of these three lithotypes is consistent with other sections of the southern limb on the Prague Synform (see Fig. 2).

(i) *Black silty-micaceous laminites* (Fig. 10A) represent claystones, densely intercalated with mainly about 0.5 mm thick, medium to poorly sorted silt laminae, which are mainly composed of subangular quartz and K-feldspar (with an albite component) grains. To a lesser extent, muscovite and framboidal pyrite, the latter infilling and/or replacing organic matter remnants, occur in silt laminae. Well-rounded zircon grains are rare in the silt laminae. In claystone intercalations *c*. 40 μm thick discontinuous laminae composed exclusively of organic matter are common, which could possibly represent either microbial mats or other compacted organic material. Moreover, authigenic TiO₂ is a common feature of the clay matrix.

Thickness of the laminites is about 70 cm starting just above the lower disconformity documented by the gap in the graptolite record (see Fig. 4). The second disconformity is developed about 30 cm above base of the laminites, and above that there are upward-fining laminites. The transition between the laminites and black shales is gradual, within about a 1 m thick interval in which sets of silty-micaceous laminae alternate with black shale. Laminites with high TOC (ca 6 wt. %), lacking any benthic body fossils or trace fossils, were deposited in an oxygen-deficient environment. In the *acuminatus* Biozone, however, two thin beds of pale mudstone (Fig. 9B) are intercalated within the laminite succession, presumably indicating temporary increases of very fine clastic material input and, perhaps, disrupted anoxia. The laminites have been interpreted by Oczlon (1992) as deposits from contour currents sweeping a sea-bottom high. This interpretation is supported by the palaeogeographical distribution of laminites in the Prague Synform and their coupling with the above-noted gaps in the sedimentary record (Štorch 2006).

(ii) *Black shales* (Fig. 10C) are present in the Hlasná Třebaň section from the upper *cyphus* Biozone, through Rhuddanian-Aeronian boundary to the lower *pectinatus* Biozone. This lithotype represents weakly laminated claystones (grainsize < 20 μm) with dispersed grains of quartz, K-

feldspar and muscovite with a maximum size of 40 μm. Discontinuous up to 5 μm thick laminae of organic matter with dispersed pyrite are common. In addition, two discontinuously zoned, authigenic barium K-feldspar grains were found, which could point to low temperature fluid alteration of the claystones. Lower Silurian graptolitic black shales, which were spread across peri-Gondwanan Europe are widely regarded as off-shore anoxic deposits. The poorly developed lamination in the Hlásná Třebaň section indicates rather continuous hemi-pelagic sedimentation without significant breaks.

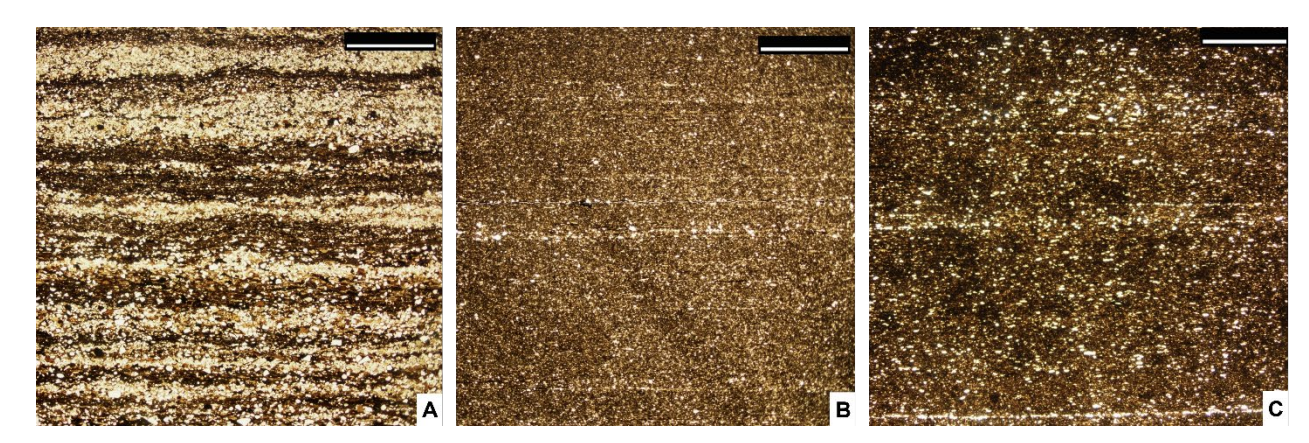


Fig. 10. Thin sections of principal lithotypes developed in the Rhuddanian-Aeronian succession at Hlásná Třebaň. **A**. Silty-micaceous laminite, *acuminatus* Biozone. **B**. Black shale, uppermost *cyphus* Biozone. **C**. Black siliceous shale, *pectinatus* Biozone. Scale bar represents 2 mm. After Štorch *et al.* (2018).

(iii) *Black siliceous and silty shales* (silty silicites, Fig. 10D) developed gradationally from the previously described lithotype in the upper part of the section shown on the log. This facies consists of couplets of about 5 cm thick siliceous shale and about 10 cm thick silty, coarsely laminated shale enriched with silica (silty silicite). The transition between these lithologies is gradual over a scale of a few milimetres. Exceptional K-feldspar and muscovite grains of a maximum size of 50 μm are dispersed in the laminated shale matrix with abundant, largely quartz grains < 20 μm. Partially recrystallized quartz grains form silica cement. Discontinuous, 15 μm thick laminae composed entirely of organic matter are common. Phosphate occurence is characterized by crandallite and churchite grains, the latter enveloped by organic matter. The origin of remobilized silica remains unclear as primary sedimentary textures are obscured by diagenetic processes. It seems linked with either recurrent periods of increased input of fine-grained clastic quartz or primary cyclicity due to periodic enrichment of sediment by biogenic silica, although no undoubted radiolarians or sponges have been found.

5c. TOC and organic carbon and nitrogen isotope geochemistry

The section was densely sampled for total organic carbon content (TOC) as well as for carbon and nitrogen isotope composition using the same regular intervals (10 cm and 5 cm) from the Silurian-Ordovician boundary to the base of the *simulans* Biozone to increase the resolution from the previous sampling over a stratigraphically wider range (from the Ordovician/Silurian boundary to the *convolutus* Biozone), presented by Frýda & Štorch (2014). The new sampling (Fig. 4) included 37 samples for nitrogen and organic carbon isotope composition and TOC. The methodology was described in Štorch *at al.* (2018).

The newly gathered data on TOC and organic carbon isotope composition (Fig. 11) confirm previously published data (Frýda & Štorch 2014), collected from another outcrop at Hlasná Třebaň, situated about 8 m SW of the proposed GSSP in its lower part (Fig. 3). Note that Frýda & Štorch (2014) did not note the presence of the upper disconformity or the occurrence of the *acuminatus* Biozone in the lower part of their section. They were following the biostratigraphical data of Štorch (2006). Therefore, a short interval between the lower and upper disconformities (i.e. samples 340–330, 330–320 and 320–310; see Fig. 4) belonging to the *acuminatus* Biozone is identical to the lithological sequence from about 5 to 40 cm above the Ordovican-Silurian boundary shown by Frýda & Štorch (2014, fig. 4) as the lower part of the *vesiculosus* Biozone.

The $\delta^{15}N$ values vary from -0.9 to 0.1% through the measured section and reveal a weak, but statistically significant decreasing trend from the *cyphus* to middle *triangulatus* Biozone, from which point the $\delta^{15}N$ values start to increase upwards to the lower part of the *pectinatus* Biozone (Fig. 12). The $\delta^{15}N$ values in higher part of the *pectinatus* Biozone seem to decrease slightly and again increase in the youngest strata (Fig. 11).

The Rhuddanian-Aeronian boundary interval exhibits no change in evolution of the nitrogen isotopic record and is characterized by $\delta^{15}N$ values of c. -0.5‰. On the other hand, the organic carbon isotope record exhibits minor but world-wide correlatable positive excursion just above the base of the *triangulatus* Biozone. The TOC content increases from the *vesiculosus* Biozone upwards and reaches its highest values close to the Rhuddanian-Aeronian boundary, from which point it significantly decreases into the overlying strata (Fig. 11).

Taken together, probably not all short-term δ^{13} C and δ^{15} N fluctuations can be traced because of the rather low rate of sedimentation at the Hlásná Třebaň section. Nevertheless, the δ^{15} N data suggest that main community of primary producers could have been the same throughout the whole studied interval. However, their identity is difficult to determine without additional data on organic chemistry (e.g., Capone *et al.* 2008). On the other hand, the TOC record revealed a

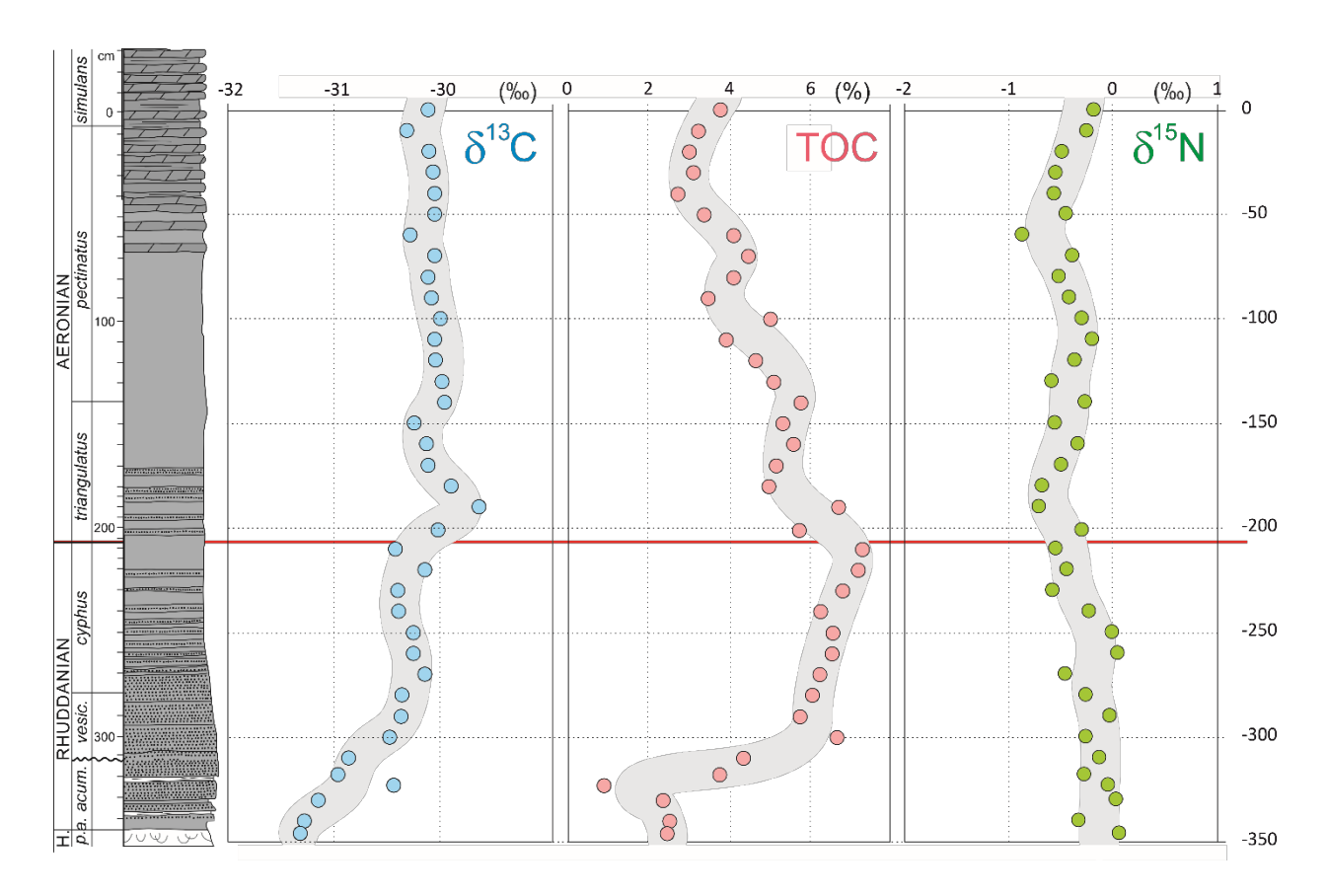


Fig. 11. C_{org} and *N*_{bulk} isotopic record in the Hlasná Třebaň section plotted with TOC. Base of the Aeronian Stage marked by red line. See Fig. 4 for lithology explanations and abbreviations. After Štorch *et al.* (2018).

distinct change at the level proposed herein to mark the base of the Aeronian Stage of the Silurian System. Rather constant TOC values of about 6 wt. % in the upper part of the Rhuddanian start to decrease significantly. It is difficult to distinguish whether the decreasing trend was caused by an increasing sedimentation rate, by decreasing of paleoproductivity, or a combination of the two. The newly gathered δ^{13} C data confirm the results of the previous study (Frýda & Štorch 2014) and show a minor positive excursion just above the base of the *triangulatus* Biozone (Fig. 11). This is correlative with early Aeronian positive excursion (EACIE) recorded in Laurentia (Melchin & Holmden 2006; Braun *et al.* 2021), Baltica (Hammarlund *et al.* 2019) and south China (Li *et al.* 2019) and further enhances correlative potential of the Hlásná Třebaň section.

5d. Redox element proxies.

Cerium anomalies can reflect the redox conditions of the overlying water column and the cerium composition of strata is resistant to changes during burial and diagenesis (Wignall 1994). The calculated Ce/Ce* values of the Hlásná Třebaň samples yielded a variation from 0.90 to 1.14 (Fig.

12). Possible correlation of the positive Ce/Ce* values with zircon accumulations in shales can be ruled out with the exception of the pale mudstone from the *acuminatus* Biozone (Fig. 12), which reached the highest positive Ce/Ce* (1.14) and the highest Zr content (364 ppm). Hence, Ce/Ce* ratios of 1.04–1.14 suggest that Rhuddanian sediments were deposited under anoxic (reducing) conditions. Certain parts of the Aeronian (Ce/Ce* = 0.90–1.07) sedimentary record (middle *triangulatus* and upper *pectinatus* biozones) could have been deposited under anoxic conditions interrupted by occasional bottom water ventilation.

Vanadium is a redox-sensitive element, the sedimentary geochemistry of which is similar to that of Ni, although subtle variations in their occurrence are capable of providing useful palaeoenvironmental information (Wignall 1994). Hence V/(V+Ni) can serve as a redox proxy (Fig. 12). Wignall (1994) reported V/(V+Ni) ratios of 1–0.83 for euxinic conditions, 0.83–0.57 for anoxic conditions, 0.57–0.46 for dysoxic conditions, and < 0.46 for oxic conditions. Both V and Ni in Hlásná Třebaň samples seem to be authigenic when compared to Ti/Al and Zr, i.e. to detrital input proxies (Fig. 12). It cannot be ruled out that V/(V+Ni) values in laminites of the *acuminatus* and *vesiculosus* biozones could be obscured by detrital input of vanadium shifting the V/(V+Ni) proxies to higher (euxinic) levels (Fig. 12). Taking into account the V/(V+Ni) values ranging from 0.90 to 0.98, the sedimentary record of the Hlásná Třebaň section could reflect deposition under euxinic conditions, which is supported by the abundant occurrence of framboidal pyrites in the laminite facies. However, the size of the framboids ranges from 5 to 10 μm in diameter which correlates with both a syngenetic origin within euxinic water column (<6 μm) and a diagenetic origin (>6 μm) within sediment (Wilkin *et al.* 1996; Wignall *et al.* 2005). A possible explanation of the occurrence of both syngenetic and diagenetic pyrite framboids could be intermittent euxinia.

The minimum V/(V+Ni) value of 0.90, representing a shift towards rather anoxic conditions, is recorded at the base of *triangulatus* Biozone, i.e. at the base of Aeronian (Fig. 12). The character of chemical conditions of deposition could be additionally examined using the V/Cr index (Jones & Manning 1994), which is also a valuable measure of palaeoredox conditions (Fig. 12). Ratios of V/Cr are in the range of 2.5–3.4 in the *acuminatus* Biozone, 4.1–5.5 in the *vesiculosus* Biozone, 4.4–9.0 in the *cyphus* Biozone, 4.4–10.3 in the *triangulatus* Biozone, 5.6–14.4 in the *pectinatus* Biozone, and 9.27 in the *simulans* Biozone. This could suggest dysoxic–anoxic conditions for the *acuminatus–vesiculosus* biozones and anoxic conditions during deposition of *cyphus–simulans* biozone sediments. However, Cr positively correlates with Ti/Al and Zr proxies and hence its concentration is not authigenic but rather dependent on detrital input, which caused a shift towards dysoxic values (2.5–4.1 of V/Cr) in the *acuminatus* and *vesiculosus* biozones and possibly lowered levels of anoxia in the other biozones. Taken together, the geochemical evidence indicates that the

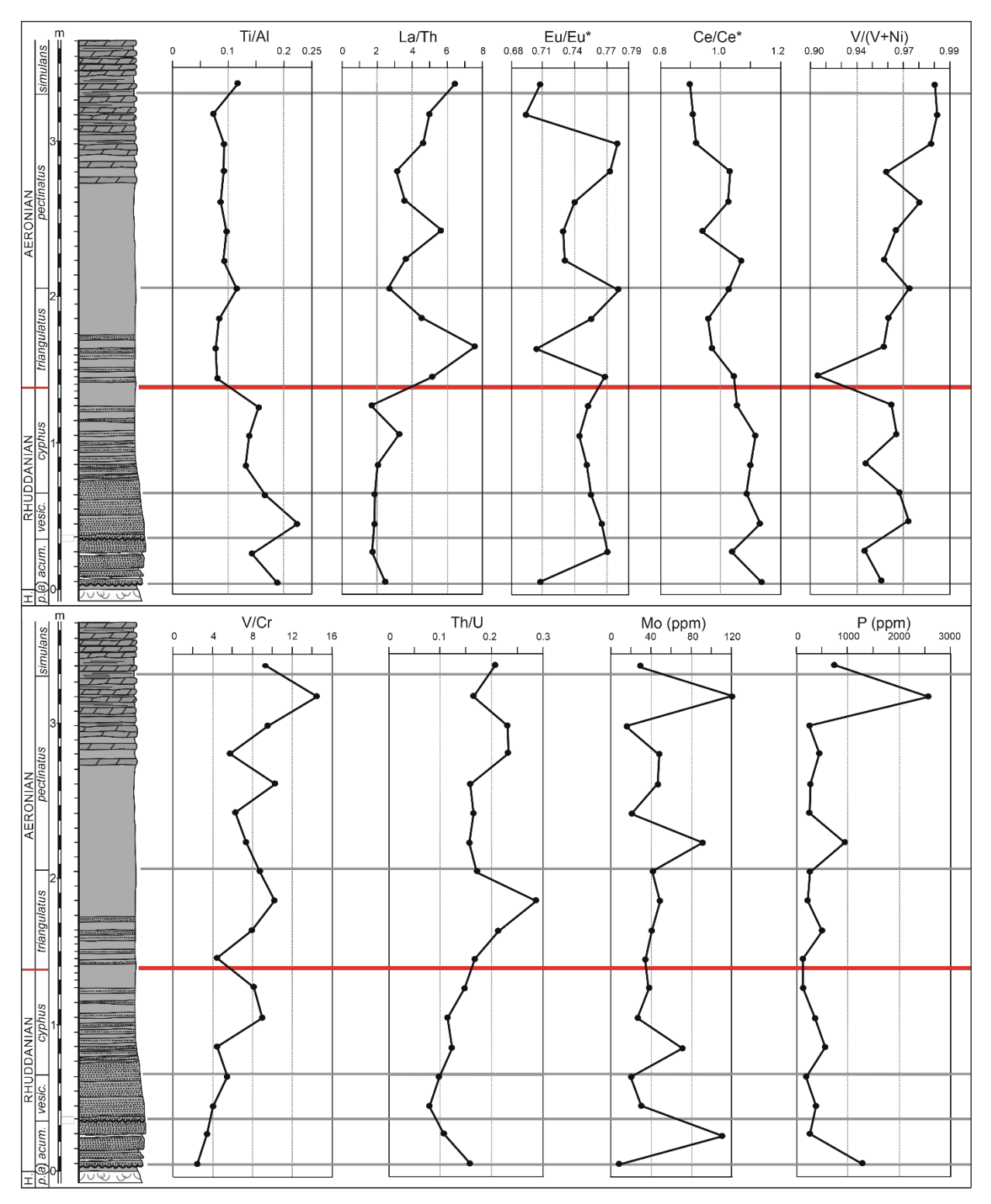


Fig. 12. Stratigraphic distribution and values of selected ratios of sedimentary proxies and redox-sensitive trace elements. Base of the Aeronian Stage marked by red line. See Fig. 4 for lithology explanations and abbreviations. After Štorch *et al.* (2018).

black shales of the Hlásná Třebaň section were deposited under anoxic or even euxinic conditions according to V/Cr ratios. The base of *triangulatus* Biozone (base of Aeronian) is marked by a change to less strongly reducing depositional conditions.

In addition, the Th/U ratio also serves as a proxy for the redox conditions of a depositional environment, distinguishing anoxia at values of Th/U < 2 (Wignall 1994; Wignall & Twitchett 1996). The black-shale succession of the Hlásná Třebaň section provided low Th/U values in the range of 0.08–0.29 (Fig. 12), which is typical for anoxic environments. The values of Th/U gradually increase from the *vesiculosus* Biozone to the upper *triangulatus* Biozone, with a marked drop at the base of the *pectinatus* Biozone. The upper part of the *pectinatus* Biozone, characterized by the onset of siliceous shales, possibly reflects a shift towards less reducing depositional conditions, yet still anoxic, as documented by the increase in Th/U, and a decrease in V/(V+Ni) and V/Cr. The *acuminatus* Biozone is marked by decreasing Th/U and V/(V+Ni) and by an increase in V/Cr, which could possibly correspond to a lesser detrital component, as suggested by the lower frequency of coarse silty laminae.

Molybdenum content (8–122 ppm) does not correlate with either V/(V+Ni) (Fig. 11) or TOC (Fig. 11) in the *acuminatus–triangulatus* biozones. However, the highest Mo contents in the shales of the *pectinatus* Biozone fit slightly better with the V/(V+Ni) and TOC curves. The latter could be explained via additional release and reduction of molybdenum from organic matter and pointing to the anoxic character of the pore waters (Calvert & Pedersen 1993). However, the lack of correlation of Mo with TOC in Rhuddanian shales and laminites and in samples from the Aeronian *triangulatus* Biozone instead indicates Mo uptake from water by authigenic sulphides, the formation of which occurs in anoxic conditions and should be most rapid under euxinic conditions (Algeo & Maynard 2004). In addition, phosphorus content (125–2546 ppm), serving as a palaeoproductivity proxy, shows a similar pattern to that of molybdenum (Fig. 12). Therefore, the shales of the *pectinatus* Biozone preserved remineralized P, which was not released into water column during decomposition of organic matter but remained immobilized in phosphatic form in shales. Conversely, decompositional phosphorus from the *acuminatus–triangulatus* biozones was likely lost into water column.

5e. Magnetic susceptibility

Magnetic susceptibility was examined in 76 whole-rock samples collected from the section using a 5 cm vertical interval. The methodology was described by Štorch *et al.* (2018). Magnetic susceptibility data show prominent decreasing trend (from values around 70 to values around 20 × 10⁻⁹m³kg⁻¹) and an oscillatory pattern in the lower and middle Rhuddanian succession beginning from the incomplete *ascensus, acuminatus* and *vesiculosus* biozones, through the *cyphus* Biozone toward the base of the Aeronian (Figure 13). In the lower part of the Aeronian succession, in the

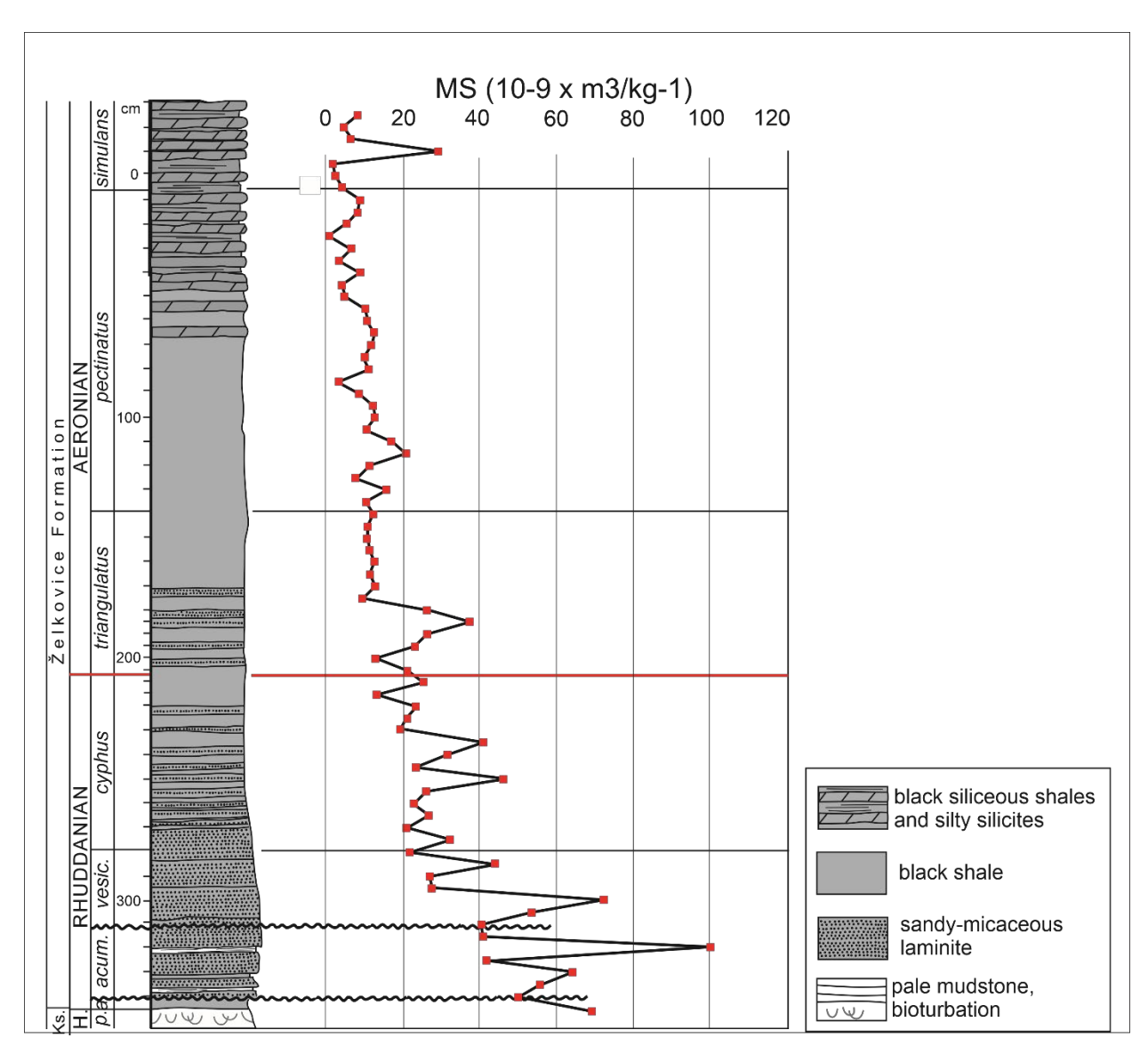


Fig. 13. Magnetic susceptibility in the Hlasná Třebaň section. Base of the Aeronian Stage marked by red line. See Fig. 4 for lithology explanations and abbreviations. After Štorch et al. (2018).

triangulatus and pectinatus biozones, MS data show quite low and uniform values without noticeable peaks or variations (average value $10.5 \times 10^{-9} \text{m}^3 \text{kg}^{-1}$). The general decreasing trend continues toward the base of the *simulans* Biozone. The MS curve through the studied section strongly reflects the gradual change in lithology. Oscillations of MS in the lower and middle Rhuddanian succession, represented by the silty-micaceous laminites in the lowermost part of the studied section, and alternating with black shales higher in the section, reflect a decreasing proportion of coarser detrital material and probably also a change in the mineralogy (a slightly increased amount of dispersed limonite). In the upper half of the *triangulatus* and lower half of the *pectinatus* biozones MS oscillations weaken, which reflects the prevailing uniform lithology of black shale with almost no silty-micaceous intercalations and laminae. A further decrease in MS in the upper part of the *pectinatus* Biozone and lowermost part of the *simulans* Biozone reflects

the increasing proportion of a diamagnetic component – quartz – in the black shales, and the lithology changing toward siliceous shales and silty silicites.

6. Biodiversity and palaeobiogeographical outline of the graptolite fauna across the Rhuddanian-Aeronian boundary

In the Prague Synform, the uppermost Rhuddanian and lowermost Aeronian beds yield a highly diverse graptolite fauna that represents a substantial proportion of global graptolite species diversity at this time. Global diversity reached a maximum of slightly more than 60 species in the early Aeronian according to Cooper *et al.* (2014). Of this total 31 species have been found in the *triangulatus* Biozone of the Hlásná Třebaň section.

(i) Among biserial and uni-biserial graptolites, the long-ranging Rhaphidograptus toernquisti predominates through the boundary interval, accompanied by slender, for the most part poorly preserved specimens of Metaclimacograptus aff. slalom and abundant Metaclimacograptus undulatus. Glyptograptids of Gl. tamariscus affinity (Glyptograptus ex gr. tamariscus) are difficult to identify confidently when unfavourably preserved. Glyptograptus perneri had its lowest occurrence 3 cm below the FAD of Dem. triangulatus in the Hlásná Třebaň section. The Rhuddanian-Aeronian boundary interval is further characterized by the incoming of the relatively common and easily identified wedge-shaped Ps. radiculatus (which has its FAD c. 10 cm below FAD of Dem. triangulatus) and the multi-spinose Ps. inopinatus (FAD c. 3 cm below the lowest Dem. triangulatus), both of which range through the triangulatus Biozone to the lower part of the pectinatus Biozone (Fig. 4). Whereas Ps. inopinatus is known from the triangulatus Biozone of northeastern Spain (Gutierrez-Marco & Štorch 1998) and probably the cyphus Biozone of the south Urals in Kazakhstan and the Arctic Canada (Koren' & Rickards 1996), the minute Ps. radiculatus occurs in Thuringia, Germany (Manck 1918, Maletz et al. 2021), Prague Synform and Hlinsko area of Bohemia (Štorch 2023, = Ps. finneyi of Štorch & Kraft 2009), the Rheidol Gorge, Wales (Melchin et al. 2023), and the Hubei (Maletz et al. 2021) and Sichuan (PS personal observation) provinces of China. Pseudorthograptus mitchelli vanished in the uppermost part of the cyphus Biozone but the robust Ps. obuti, which occurs from the Urals through Lithuania, Norway, Thuringia, and Bohemia to Morocco and also Myanmar, survived into the lowermost triangulatus Biozone (c. 8 cm above the base in Hlásná Třebaň) where it is replaced by Petalolithus ovatoelongatus – the rather cosmopolitan earliest representative of the genus Petalolithus occuring at least across peri-Gondwana, Avalonia and Baltica. The stratigraphically highest specimens of the robust *Neodiplograptus fezzanensis*, rarely found in the *triangulatus* Biozone, precede the

advent of the closely similar *Neodiplograptus magnus* in the middle *triangulatus* Biozone. *Nd. fezzanensis* represents a typical element of the Gondwanan and peri-Gondwanan realm (Algeria, Bohemia, Libya, Morocco, Niger, Spain; Štorch & Massa 2003) in the *cyphus* Biozone whereas *Nd. magnus* is an abundant biozonal index species in the Welsh Basin and other parts of Britain (Toghill 1968; Zalasiewicz & Tunnicliff 1994; Zalasiewicz *et al.* 2009; Melchin *et al.* 2023). In the Welsh Basin, however, *Nd. magnus* had its lowest occurrence much higher than in the Prague Synform, above the FAD of *Demirastrites fimbriatus* (Nicholson), which is a junior synonym of *Demirastrites pectinatus* (Richter) as cited in this paper.

(ii) Monograptid graptolites (uniserial taxa) underwent remarkable diversification and evolutionary progress through the Rhuddanian-Aeronian boundary interval. The almost simultaneous appearance of several genera with novel isolated and hooked triangular thecae (Fig. 5D, G, H, J, L–N, P: *Demirastrites, Rastrites, Campograptus*) has a good potential for global biostratigraphical correlation despite the fact that few of the individual species may be regarded as truly cosmopolitan. As more morphological information emerges, closely similar and related species, formerly regarded as a single cosmopolitan taxon tend to be confined in marine basins and oceans around different continents (Sun *et al.* 2022). In the Prague Synform and the Hlásná Třebaň section itself, the base of the Aeronian succession is clearly marked by the advent of *Dem. triangulatus* – the earliest species with isolated high-triangular thecae furnished with laterally extended apertural horns. The species is widely distributed in peri-Gondwana, Avalonia and Baltica. Its occurrence in circum-equatorial province of Melchin (1989), comprising North America, Siberia and China, need further examination although Maletz *et al.* (2021) stated that their specimens from Hubei, China closely match early form of *Dem. triangulatus* recognized by Štorch & Melchin (2018) in Bohemia.

Uppermost Rhuddanian strata can be distinguished by abundant and easily recognizable rhabdosomes of the biozonal index C. *cyphus*, associated with early populations of *Coronograptus gregarius*, abundant *Pernerograptus sudburiae* (formerly assigned to *Monograptus argutus* by Bouček 1953 and Štorch 1994) and the common, robust *Pernerograptus difformis* with high-triangular mesial thecae. *Coronograptus cyphus* disappears 1–2 cm below, and *Pern. difformis c.* 3 cm above the lowest *Dem. triangulatus. Pernerograptus revolutus* is also confined to the boundary interval. *Pernerograptus* sp. nov. (Fig. 4K), readily distinguished by its crook-shaped rhabdosome with few triangular mesial thecae and rather short proximal part, has been detected 1–3 cm below the boundary. This form is a striking element of the graptolite assemblage of the uppermost *cyphus* Biozone in Spanish sections (PS, personal observation). Rhabdosomes questionably assigned to *Pernerograptus sequens* have been recorded in several samples of the

triangulatus Biozone beginning 2 cm above the base of the Rhuddanian succession. This species, confined to middle part of the triangulatus Biozone in Wales (Zalasiewicz et al. 2009), was further reported by Bjerreskov (1975) from upper triangulatus and lower pectinatus subzones of the Coronograptus gregarius Biozone of Bornholm (Denmark). Rastrites longispinus (the stratigraphically lowest species of Rastrites in Europe), Demirastrites brevis and Campograptus rostratus had their lowest occurrences 20 cm above the base of the Aeronian succession in the Hlásná Třebaň section, still in the lower third of the triangulatus Biozone. Rastrites longispinus is widespread in the triangulatus and pectinatus biozones of the broader European realm (peri-Gondwana, Avalonia and Baltica).

The present results and evaluation of published data have shown that high-resolution correlation of the Hlásná Třebaň section will be easy and straightforward with sections in the Prague Synform and those from Morocco, Portugal and Spain through Italy, Serbia, Bulgaria and Turkey in the south across central Europe to the east Baltic countries, Sweden, Denmark and Britain in the north. Although the lowest occurrence of *Dem. triangulatus* is a good anchor for any intercontinental biostratigraphical correlation, high-resolution correlation of the European graptolite sequence with those of North America, Siberia and China would benefit from further, world-wide systematic revisions of respective faunas.

7. Readily correlatable Rhuddanian-Aeronian boundary strata worldwide

Anoxic black shales rich in planktic graptolites are particularly widespread in the lowermost Silurian (Melchin *et al.* 2013) and the same litho- and bio-facies continued through the Rhuddanian-Aeronian boundary interval in many parts of the world.

Britain. – A continuous sequence of Rhuddanian-Aeronian boundary strata crops out in the Rheidol Gorge, east of Aberystwyth in mid Wales. The succession alternates between grey bioturbated mudstones in which graptolites are uncommon and black shales with a common and highly diverse graptolite fauna of the *C. cyphus* and *Dem. triangulatus* biozones. Although the rocks are cleaved and low-grade metamorphosed, both graptolites and associated chitinozoans of the *Spinachitina maennili* Biozone are moderately to well-preserved (Melchin *et al.*, 2023). Sudbury (1958) published a list of graptolite taxa recorded from her *gregarius* Biozone, which roughly corresponds with the *Dem. triangulatus*, *Nd. magnus* and *Prib. leptotheca* biozones of Zalasiewicz *et al.* (2009) and Loydell (2012). The graptolite fauna has been revised and Sudbury's identifications reassessed by Melchin *et al.* (2023) in their detailed study of the Rheidol Gorge

section. *Petalolithus ovatoelongatus* appears well above the lowest *Dem. triangulatus* and *R. longispinus* is reported from the *Neodiplograptus magnus* Biozone in association with *Dem. pectinatus* (= *fimbriatus*) and *Camp. communis* similarly as in Bohemia. A similar pattern of species occurrence through the boundary interval has been also recorded in *Ps. radiculatus*, *Pr. concinnus* and several other species common with the Hlásná Třebaň section. The Rheidol Gorge section is also being proposed to the ISSS voting members as another candidate for the replacement Rhuddanian-Aeronian GSSP (Melchin *et al.* 2016, 2023).

Toghill (1968) described the lower and middle Llandovery succession of the Birkhill Shales at Dob's Linn near Moffat, southern Scotland. He recognized the upper Rhuddanian *cyphus* Biozone, which is closely comparable to the *cyphus* Biozone applied here. The black mudstones of the *cyphus* Biozone are separated by ca 0.3 m thick graptolite-barren claystone with calcareous nodules from the overlying black mudstones of the *gregarius* Biozone. The base of the *gregarius* Biozone is marked by the lowest occurrence of *Dem. triangulatus* s.l. whereas *C. gregarius* is reported from as low as the middle *cyphus* Biozone. The *gregarius* Biozone of Toghill, however, includes in its upper part an interval with *Dem. pectinatus* (the senior name to *M. fimbriatus*) and *Nd. magnus*. The Dob's Linn succession requires more detailed study for a full systematic documentation of its Rhuddanian-Aeronian graptolite faunas.

Central, Western and Southern Europe, Northwestern Peri-Gondwana. — A rather condensed and tectonized succession of hemipelagic black clayey and siliceous shales and cherts with abundant graptolites occurs in Thuringia and Vogtland, Germany. The Rhuddanian-Aeronian boundary beds have been described from several sections near Ronneburg and Hohenleuben by Schauer (1971). The graptolite fauna appears to be closely related to that of the Bohemian sections but detailed comparison suffers from the effects of tectonic strain on the Thuringian graptolites. The uppermost Rhuddanian strata belong to the cyphus Biozone. The lower Aeronian gregarius Biozone is marked by common Dem. triangulatus associated with Dem. pectinatus. However, some graptolite occurrences, such as that of Petalolithus minor in the middle cyphus Biozone, and C. cyphus, H. acinaces and Pern. difformis from the lower triangulatus Biozone call for further field work and taxonomic examination of the fauna.

Graptolite-bearing black-shale sections through Rhuddanian-Aeronian boundary strata have also been recorded in the Carnic Alps (Oberbuchach section of Jaeger & Schönlaub 1980) and in the Seville Province of Spain (sections around El Pintado reservoir in Valle Syncline, Jaeger & Robardet, 1979). Both sections are in need of more detailed work to be correlated with proper resolution.

Northeastern Europe, sections located on Baltica. – Rhuddanian-Aeronian boundary strata, which are unfavourably exposed on Bornholm, were described in the comprehensive graptolite paper by Bjerreskov (1975). The poorly exposed upper Rhuddanian succession was assigned to the *Pern. revolutus* Biozone since *C. cyphus* is very rare on Bornholm and in Sweden. The lowermost Aeronian was referred to the *gregarius* Biozone, the base of which is indicated by the almost simultaneous lowest occurrences of *C. gregarius* and *Dem. triangulatus* s.s. Accordingly, Bjerreskov (1975) divided her *gregarius* Biozone into a lower *triangulatus* Subzone and upper *pectinatus* Subzone, which both match with biozones as applied in Bohemia. The FAD of *Pet. ovatoelongatus* closely follows that of *Dem. triangulatus* whereas *R. longispinus* debuts somewhat higher, in the upper part of the *triangulatus* Subzone. Loydell *et al.* (2017) described the Rhuddanian-Aeronian boundary interval in the Sommerode-1 borehole situated near the section studied by Bjerreskov (1975). They recognized *Pern. revolutus* Biozone in the uppermost Rhuddanian, followed by the *triangulatus* Biozone in the lowermost part of the Aeronian succession. Reassessed graptolite assemblages closely resemble those reported from Bohemia, including the successive appearance of principal marker species.

Waern (1960) reported graptolite-bearing Rhuddanian-Aeronian boundary beds from the Silvberg Section in Dalarna, Sweden, with a rather condensed upper Rhuddanian *revolutus* Zone overlain by the *gregarius*, *folium*, *cometa* and *sedgwickii* biozones of the Aeronian Stage.

The subsurface extent of upper Rhuddanian and Aeronian mudrocks with graptolites and chitinozoans has been documented in numerous drill cores in Latvia and Lithuania. The moderate diversity graptolite fauna of the *cyphus* and *triangulatus* zones, described by Paškevičius (1979), exhibits close similarity to that of peri-Gondwanan Europe, after some taxonomic reassessment. The middle and upper parts of the *triangulatus* Biozone in the sense of Paškevičius (1979), however, correspond with *pectinatus*, *simulans* and perhaps also *leptotheca* biozones of Štorch (2006) and herein. Several marker species of the *leptotheca* Biozone, including *Campograptus millepeda* and *Petalolithus folium* have been reported from the upper *triangulatus* Biozone of Lithuania by Paškevičius. The suggested base of the Aeronian Stage and the whole *triangulatus* graptolite Biozone correlate with a level within the *Aspelundia expansa* conodont Biozone as shown by the integrated graptolite and conodont data from the Aizpute-41 core, Latvia (Loydell *et al.* 2003).

China, Yangtze Platform. – A large number of richly fossilliferous sections across the Rhuddanian-Aeronian boundary interval is available on the Chinese Yangtze Platform. Detailed knowledge of these sections is lacking since earlier authors focused on the late Rawtheyan and Hirnantian

succession and Ordovician-Silurian boundary interval in particular. Rhuddanian-Aeronian boundary strata are within the rather uniform, offshore, black shale succession of the lower and middle Llandovery Lungmachi (or Longmaxi) Formation all over the Yangtze Platform (Fan *et al.* 2011).

Chen & Lin (1978) defined a "Pristiograptus" cyphus – "Monoclimacis" lunata Biozone in the upper Rhuddanian of the Tongzi area of the northern Guizhou Province. The rich graptolite assemblage of the biozone, however, included genera typical of Aeronian strata elsewhere in the world (Petalolithus, Rastrites and triangulate monograptids of Dem. triangulatus affinity). Hence the base of the Aeronian Stage likely occurs within the cyphus—lunata Biozone of Chen & Lin (1978). The C. gregarius Biozone as recognized in the lower Aeronian succession, was divided into the lower Rastrites guizhouensis and upper Dem. triangulatus subzones. Graptolite assemblages are markedly different from those of Baltica, Avalonia and peri-Gondwanan Europe in species represented and in the relative diversity and abundance of the genera.

Ni (1978) studied the graptolites of the Lungmachi Formation from the Yichang (Yangtze Gorges) area of the western Hubei Province. The level of the Rhuddanian-Aeronian boundary is unclear, however, as *Rastrites* (*R. cirratus* Ni) was reported from as low as the upper Rhuddanian *Pristiograptus leei* Biozone, whilst monograptids of the *Dem. triangulatus* group were missing in the lower Aeronian *triangulatus* Biozone of Ni (1978). Wang (1985) reported *Dem. triangulatus* from the Yangtze Gorges region and reconciled the Rhuddanian and Aeronian graptolite biozonation of the area with the international standard (see Loydell 2012), although notable differences in graptolite faunas did not allow for high resolution correlation with European sections.

Rhuddanian and Aeronian black shales of the Lungmachi Formation exposed in Guanyinqiao, in Qijiang District of Sichuan Province were documented by Jin et al. (1982). Both sedimentary rocks and graptolite fauna are consistent with those encountered in other regions of south-central China. The *C. cyphus* and *P. leei* biozones have been recognized in the upper Rhuddanian while the lower Aeronian commenced with the *triangulatus* Biozone, overlain by the *Camp. communis* Biozone. The base of the Aeronian is marked by the FAD of *Dem. triangulatus* followed by abundant rastritids. *Petalolithus palmeus qijiangensis* Zhao, reported from the uppermost Rhuddanian *leei* Biozone, which closely resembles the robust rhabdosomes of *Pseudorthograptus obuti* or *Ps. mutabilis*.

In connection with the current search for a new Aeronian GSSP, the well-exposed hemipelagic black shales of the Rhuddanian-Aeronian boundary interval, rich in well-preserved graptolites and chitinozoans, have been studied in Shuanghe and Yuxian sections in southern

Sichuan (authors' unpublished data) and in Shennongjia anticline in northwestern Hubei (Maletz et al. 2021). A probable gap in sedimentation at the base of the *triangulatus* Biozone is indicated in the latter section by sudden and simultaneous appearance of a number of taxa incoming together with the lowest *Dem. triangulatus*. Shao et al. (2018) proposed the Liangshan Danangou section in southern Shaanxi as possible stratotype section but Štorch & Melchin (2018) noted that their only illustrated specimen of *Dem. triangulatus* does not belong to this species.

Siberia. – Silty shales rich in upper Rhuddanian and lower Aeronian graptolites were documented by Sennikov (1976) from several sections in the Gorny Altai, although the Rhuddanian-Aeronian boundary interval has never been studied in particular detail in this region. A Dem. triangulatus Biozone overlying the upper Rhuddanian cyphus Biozone witnessed the FADs of triangulate monograptids, petalolithids and rastritids. However, specimens assigned by Sennikov (1976) to Dem. pectinatus are confined to the lower part of the triangulatus Biozone as opposed to European records of the species which come for the most part from above the range of Dem. triangulatus. Subsequent revision based upon the richly fossiliferous reference section near Ust-Chagirka (Obut & Sennikov 1985) introduced the triangulatus-gregarius Biozone embracing all Aeronian strata up to the base of L. convolutus-Ceph. cometa Biozone. In the Voskresenka-4 section in Gorny Altai, described by Sennikov et al. (2008), Dem. triangulatus first occurs above the LAD of C. cyphus, and the first appearances of Rastrites and Camp. communis occur just above that of Dem. triangulatus, a pattern similar to that seen at Hlásná Třebaň, so this may be the most complete Rhuddanian-Aeronian boundary section in the region.

Numerous drill cores running through Rhuddanian-Aeronian boundary strata were documented by Obut *et al.* (1968) from the Norilsk area (southwestern Siberian Platform). The lower Silurian succession, which rests unconformably on middle Ordovician shales and/or limestones, begins with dark grey calcareous shales of the upper Rhuddanian *cyphus* Biozone and/or lower Aeronian *triangulatus* Biozone. The Rhuddanian-Aeronian boundary was recorded in nine boreholes. The rich and well-preserved graptolite faunas described by Obut *et al.* (1968) exhibit some similarity in species composition and relative abundance to faunal assemblages of the Yangtze Platform although no attempt has been made for rigorous comparison. No actual specimens of *C. cyphus* were recorded in the *cyphus* Assemblage Biozone. The base of the Aeronian is marked by the almost simultaneous lowest occurrences of *Demirastrites* (specimens assigned to *Dem. triangulatus* and *Dem. pectinatus* by the latter authors), *C. gregarius* and *Pet. ovatoelongatus*, closely followed by *R. longispinus* and "*Stavrites*" rossicus Obut & Sobolevskaya. *Campograptus* debuts in the stratigraphically higher part of the *triangulatus* Biozone.

Northern Canada. – The Rhuddanian-Aeronian successions of dark grey to black calcareous shales with thin limestone interbeds exposed on Cornwallis Island, Nunavut were documented by Melchin (1989). New data pertaining specifically to the Rhuddanian-Aeronian boundary interval were presented by Melchin & MacRae (2014). Boundary strata are marked by a sequence of closely spaced FADs of *Pr. concinnus*, *Dem. triangulatus* and *Petalolithus* sp. The base of the *triangulatus* Biozone coincides with weak positive shift in $\delta^{13}C_{org}$ values detected by Melchin & Holmden (2006).

Black shales of the Rhuddanian-Aeronian boundary interval exposed in northern Canadian Cordillera of Yukon and Northwest Territories were documented by Lenz (1979). The uppermost Rhuddanian was assigned to the *gregarius* Biozone, which is overlain by the lowermost Aeronian *triangulatus* Biozone. Description of the sections from Peel River area has been provided by Melchin in Strauss *et al.* (2020). The base of the *triangulatus* Biozone was defined by the lowest occurrence of *Demirastrites*. The graptolite fauna described by Lenz (1982) exhibits notable similarity to likely coeval assemblages of China (Yangtze Platform) and Cornwallis Island of the Canadian Arctic.

••

8. Suitability of the Hlásná Třebaň section as a base Aeronian GSSP

The section proposed as new GSSP, located near Hlásná Třebaň village fulfils almost all of the requirements for boundary stratotype listed by Cowie *et al.* (1986) and Salvador (1994) as reviewed by the following checklist. All critical GSSP attributes are present.

The Hlásná Třebaň section
Yes (with respect to the facies)
Yes (the only gaps are down the section in
the vesiculosus and acuminatus biozones)
Low
Yes
Yes
Yes (abundant, high-diversity, well-preserved
planktic graptolites, less well-preserved
chitinozoans
Yes (uniform facies and lithology)
Yes (abrupt change of lithology 1.38 m below
the proposed boundary)
Yes
No (but the black shales may be suitable for Re-
Os dating)
No (no data obtained to date, but thermal
alteration is low)
Yes (δ ¹³ Corg isotope record with minor positive
excursion just above the boundary level)
Yes (if elected)
Yes (open access year-round)
Yes (located in Bohemian Karst Protected
Landscape Area)

9. Summary

We propose the Hlásná Třebaň section as a GSSP for the base of the Aeronian – the second stage of the Silurian System – at the point marked by the lowest occurrence of *Demirastrites triangulatus*, which also defines the base of the *Dem. triangulatus* graptolite Biozone. Data from Bohemia and an overview of published records worldwide have demonstrated that *Dem. triangulatus* is a readily identifiable and widely applicable tool for stratigraphical correlation. The FAD of *Dem. triangulatus* occurs 1.38 m above the base of Silurian black shale succession of the Želkovice Formation, just below a minor positive shift in $\delta^{13}C_{org}$ values recorded in the lower part of the *triangulatus* Biozone and recognized in many other parts of the world (e.g., Braun *et al.*, 2021). The lower *triangulatus* Biozone clearly exhibits a rapid graptolite diversification event of sudden successive appearance of several new lineages: monograptids with isolated and hooked thecae (genera *Demirastrites, Rastrites* and *Campograptus*) and *Petalolithus* with its ancorate biserial rhabdosome, tabular in cross section. The graptolite succession can be readily correlated worldwide as opposed to that of the current stratotype in the Welsh Basin.

Sedimentation within the boundary interval is continuous, without any facies change. The abundant, diverse and readily identifiable graptolite faunas are present in almost all Aeronian and Rhuddanian strata, including all strata in the boundary interval. Chitinozoans of the *maennili* chitinozoan Biozone occur in the Rhuddanian-Aeronian boundary interval. There are no significant structural complexities in the stratigraphical succession comprising the upper Hirnantian, Rhuddanian and lower and middle Aeronian (*A. ascensus – L. convolutus* biozones) exposed on this hill slope locality. The section lies within Bohemian Karst Protected Landscape Area. Both study and access by a narrow foot path uphill from the Hlásná Třebaň – Rovina road are unrestricted. Hlásná Třebaň is readily accessible by car and train from Prague in a half an hour. Other Bohemian sections spanning the Rhuddanian-Aeronian boundary interval (Karlík, Vočkov near Karlštejn, Zadní Třebaň, Černošice and Nové Butovice) archive sedimentary and graptolite records fully consistent with those described from the proposed stratotype.

Acknowledgements: The authors greatly appreciate the financial support provided by the Czech Science Foundation through projects 14-16124S and 20-23363S. PS and LC appreciate subsequent indoor support received from the Institute of Geology of the CAS (RVO 67985831). MJM acknowledges financial support from the Natural Sciences and Engineering Research Council of Canada. We are indepted to V. Turek and L. Váchová (National Museum, Prague) who photographed the shale slab (Fig. 6).

References

- Aïfa, T., Pruner, P., Chadima, M., Štorch, P. 2007: Structural evolution of the Prague Synform (Czech Republic) during Silurian times: an AMS, rock magnetism, and palaeomagnetic study of the Svatý Jan pod Skalou dikes. *In* Linnemann, U., Nance, R.D., Kraft, P., Zulauf, G. (eds) The Evolution of the Rheic Ocean: From Avalonian–Cadomian Active Margin to Alleghenian–Variscan Collision. *Special Papers–Geological Society of America* 423, 249–265.
- Algeo, T.J. & Maynard, J.B. 2004: Trace-element behavior and redox facies in core shales of Upper Pennsylvanian Kansas-type cyclothems. *Chemical Geology* 206, 289–318.
- Bjerreskov, M. 1975: Llandoverian and Wenlockian graptolites from Bornholm. *Fossils and Strata* 8, 1–94.
- Brenchley, P.J. & Štorch, P. 1989: Environmental changes in the Hirnantian (upper Ordovician) of the Prague Basin, Czechoslovakia. *Geological Journal* 24(3), 165–181.
- Bouček, B. 1953: Biostratigraphy, development and correlation of the Želkovice and Motol Beds of the Silurian of Bohemia. *Sborník Ústředního ústavu geologického, Oddil paleontologický* 20, 421–84.
- Braun, M. G., Daoust, P. & Desrochers, A. 2021: A sequential record of the Llandovery $\delta^{13}C_{carb}$ excursions paired with time-specific facies: Anticosti Island, eastern Canada. *Palaeogeography, Palaeoclimatology, Palaeoecology* 578, 110566.
- Butcher, A. 2016: Chitinozoan data from the Hlásná Třebaň section, Czech Republic a potential replacement GSSP for the base of the Aeronian stage (Llandovery Series, Silurian). 29. In Guerdebeke, P., De Weirdt, J., Vandenbroucke, T. R. A. & Cramer, B. D. (eds), *IGCP 591 The Early to Middle Paleozoic Revolution, Closing Meeting, Ghent University, Belgium, 6–9 July 2016, Abstracts*, 134pp.
- Calvert, S.E. & Pedersen, T.F. 1993: Geochemistry of Recent oxic and anoxic marine sediments: implications for the geological record. *Marine Geology 113*, 67–88.
- Capone, D., Bronk, D., Mulholland, M. & Carpenter E. (eds) 2008. Nitrogen in the Marine Environment, 2nd Edition, Elsevier, 1757 pp., ISBN: 9780123725226
- Chen Xu & Lin Yaokun, 1978: Lower Silurian graptolites from Tongzi, northern Guizhou. *Memoir of the Nanjing Institute of Geology and Palaeontology, Academia Sinica 12*, 1–106. [in Chinese with English Abstract]
- Chlupáč, I. Havlíček, V., Kříž, J., Kukal, Z. & Štorch, P. 1998. Palaeozoic of the Barrandian (Cambrian to Devonian), Czech Geological Survey, 183 pp.
- Cocks, L.R.M., Woodcock, N.H., Rickards, R.B., Temple, J.T. & Lane, P.D. 1984: The Llandovery Series of the Type Area. *Bulletin of the British Museum (Natural History), Geology Series 38*, 131–182.
- Cocks, L.R.M. & Torsvik, T.H. 2002: Earth geography from 500 to 400 million years ago: a faunal and paleomagnetic review. *Journal of Geological Society 159*, 631–644.
- Cocks, L.R.M. & Torsvik, T.H. 2006: European geography in a global context from the Vendian to the end of Palaeozoic. In Gee, D.G., Stephenson, R.A. (eds), European Lithosphere Dynamics. *Geological Society Memoirs* 32, 83–95.

- Cocks, L.R.M. & Torsvik, T.H. 2013: New global palaeogeographical reconstructions for the Early Palaeozoic and their generation. In Harper, D.A.T. & Servais, T. (eds), Early Palaeozoic Biogeography and Palaeogeography. *Geological Society Memoirs* 38, 5–24.
- Cooper, R.A., Sadler, P.M., Munnecke, A. & Crampton, J.S. 2014: Graptolite evolutionary rates track Ordovician-Silurian global climate change. *Geological Magazine 151*, 349-364.
- Cowie, J.A., Ziegler, W., Boucot, A.J., Bassett, M.G. & Remane, J. 1986: Guidelines and statuses of the International Commission on Stratigraphy (ICS). *Courier Forschungsinstitut Senckenberg* 83, 1–14.
- Cramer, B.D., Brett, C.E., Melchin, M.J., Männik, P., Kleffner, M.A., McLaughlin, P.I., Loydell, D.K., Munnecke, A., Jeppsson, L., Corradini, C., Brunton, F.R. & Saltzman, M.R. 2011: Revised correlation of Silurian Provincial Series of North America with global and regional chronostratigraphic units and δ¹³ Ccarb chemostratigraphy. *Lethaia* 44, 185–202.
- Davies, J.R., Waters, R.A., Zalasiewicz, J.A., Molyneux, S.G., Vandenbroucke, T.R.A. & Williams, M. 2010: A revised sedimentary and biostratigraphical architecture for the type Llandovery and Garth areas, central Wales: a field guide. British Geological Survey Open Report, OR/10/037.
- Davies, J.R., Waters, R.A., Molyneux, S.G., Williams, M., Zalasiewicz, J.A., Vandenbroucke, T.R.A. & Verniers, J. 2013: A revised sedimentary and biostratigraphical architecture for the Type Llandovery area, Central Wales. *Geological Magazine 150*, 300–332.
- De Weirdt, J., Vandenbroucke, T.R.A., Cocq, J., Russell, C., Davies, J.R., Melchin, M. & Zalasiewicz, J. 2019: Chitinozoan biostratigraphy of the Rheidol Gorge section, central Wales, UK: A GSSP replacement candidate section for the Rhuddanian-Aeronian boundary. *Papers in Palaeontology* 6(2), 173-192.
- Dufka, P. & Fatka, O. 1993: Chitinozoans and acritarchs from the Ordovician-Silurian Boundary of the Prague Basin, Czech Republic. *Special Papers in Palaeontology 48*, 17–28.
- Dufka, P., Kříž, J. & Štorch, P. 1995: Silurian graptolites and chitinozoans from the Uranium Industry boreholes drilled in 1968-1971 (Prague Basin, Bohemia). *Bulletin of the Czech Geological Survey*, 70, 5–13.
- Ebbestad, J., Ove, R., Frýda, J., Wagner, P.J., Horný, R.J., Isakar, M., Stewart, S., Percival, I.G., Bertero, V., Rohr, D.M., Peel, J.S., Blodgett, R.B. & Högström, A.E.S. 2013: Biogeography of Ordovician and Silurian gastropods, monoplacophorans and mimospirids. In Harper, D.A.T. & Servais, T. (eds), Early Palaeozoic biogeography and palaeogeography. *Geological Society Memoirs* 38, 199–220.
- Eriksson, M.E., Hints, O., Paxton, H. & Tonarová, P. 2013: Ordovician and Silurian polychaete diversity and biogeography. In Harper, D.A.T. & Servais, T. (eds), Early Palaeozoic biogeography and palaeogeography. *Geological Society Memoirs* 38, 265–272.
- Fatka, O. & Mergl, M. 2009: The "microcontinent" Perunica: status and story 15 years after conception. In Bassett, M.G. (ed.), Early Palaeozoic Peri-Gondwana Terranes: New Insights from tectonics and Biogeography. *Geological Society, London, Special Publications 325*, 65–101.
- Fan Jun-xuan, Melchin, M.J., Chen Xu, Wang Yue, Zhang Yuandong, Chen Qing, Chi Zhaoli & Chen Feng 2011: Biostratigraphy and geography of the Ordovician-Silurian Lungmachi black shales in South China. *Science China*; *Earth Sciences 54*, 1854–1863.

- Frýda, J. & Štorch, P. 2014: Carbon isotope chemostratigraphy of the Llandovery in northern peri-Gondwana: new data from the Barrandian area, Czech Republic. *Estonian Journal of Earth Sciences* 63, 220–226.
- Goldman, D., Maletz, J., Melchin, M.J. & Fan Junxuan 2013: Graptolite palaeobiogeography. *In* Harper, D.A.T. & Servais, T. (*eds*), Early Palaeozoic biogeography and palaeogeography. *Geological Society Memoirs* 38, 415–428.
- Grahn, Y. 1985: Llandoverian and early Wenlockian Chitinozoa from southern Ohio and northern Kentucky, USA. *Palynology* 9(1), 147-164.
- Grahn, Y. 1988: Chitinozoan stratigraphy in the Ashgill and Llandovery. *Bulletin of the British Museum, Natural History. Geology 43*, 317-323.
- Grahn, Y., 1995. Lower Silurian Chitinozoa and biostratigraphy of subsurface Gotland. *GFF* 117(2), 57-65.
- Gutierrez-Marco J.C. & Štorch, P. 1998: graptolite biostratigraphy of the Lower Silurian (Llandovery) shelf deposits of the Western Iberian Cordillera, Spain. *Geological Magazine* 135, 71–92.
- Hammarlund, E.U., Loydell, D.K., Nielsen, A.T. & Schovsbo, N.H. 2019: Early Silurian δ¹³C excursions in the foreland basin of Baltica, both familiar and surprising. *Palaeogeography, Palaeoclimatology, Palaeoecology* 526, 126–135.
- Havlíček, V., Vaněk, J. & Fatka, O. 1994: Perunica microcontinent in the Ordovician (its position within the Mediterranean Province, series division, benthic and pelagic associations). Sborník geologických věd, Geologie 46, 23-56.
- Holland, C.H. & Bassett, M.G. 1989: A global standard for the Silurian system. *National Museum of Wales Geological Series 10*, 1–325.
- Horný, R. 1956: Zóna *Akidograptus ascensus* v jižním křídle barrandienského siluru. *Věstník Ústředního ústavu geologického 31*, 62–69. [in Czech]
- Jaeger, H. & Robardet, M. 1979: Le Silurien et le Dévonien basal dans le Nord de la Province de Séville (Espagne). Géobios *12*, 687–714.
- Jaeger, H. & Schönlaub, H.-P. 1980: Silur und Devon nördlich der Gundersheimer Alm in den Karnischen Alpen (Österreich). *Carinthia II 170(90)*, 404–444.
- Jin Chuntai, Ye Shaohua, He Yuanxiang, Wan Zhengquan, Wang Shubei, Zhao Yuting, Li Shanji, Xu Xingqi & Zhang Zhenggui 1982: *The Silurian Stratigraphy and Paleontology in Guanyinqiao, Qijiang, Sichuan*. People's Publishing House of Sichuan, Chengdu. 84pp.
- Jones, B. & Manning, D.A.C. 1994: Comparison of geochemical indices used for the interpretation of palaeoredox conditions in ancient mudstones. *Chemical Geology 111*, 111–129.
- Kodym, O., Bouček, B. & Šulc, J. 1931: Guide to the geological excursion to the neighbourhood of Beroun, Koněprusy and Budňany. *Knihovna Státního geologického ústavu Československé republiky 15*, 1–83. [In Czech]
- Koren', T.N. & Rickards, R.B. 1996: Taxonomy and evolution of Llandovery biserial graptoloids from the sourthern Urals, western Kazakhstan. *Special Papers in Palaeontology 54*, 1–103.
- Kříž, J. 1975: Revision of the Lower Silurian stratigraphy in central Bohemia. *Věstník Ústředního Ústavu geologického 50*, 275–283.
- Kříž, J. 1992: Silurian field excursions: Prague Basin (Barrandian), Bohemia. *National Museum Wales, Geological Series 13*, 1–111.

- Kříž, J. 1998: Silurian. 79–101. In: Chlupáč, I., Havlíček, V., Kříž, J., Kukal, Z. & Štorch, P. (Eds.), *Paleozoic of the Barrandian (Cambrian to Devonian*). Český geologický ústav, Praha.
- Kröger, B. 2013: Cambrian–Ordovician cephalopod palaeogeography and diversity. In Harper, D.A.T. & Servais, T. (eds), Early Palaeozoic biogeography and palaeogeography. *Geological Society Memoirs* 38, 429–448.
- Krs, M. & Pruner, P. 1995: Palaeomagnetism and palaeogeography of the Variscan formations of the Bohemian Massif, comparison with other European regions. *Journal of Geosciences 40*, 3–46.
- Krs, M. & Pruner, P. 1999: To the paleomagnetic investigations of paleogeography of the Barrandian Terrane, Bohemian Massif. *Acta Universitatis Carolinae, Geologica* 43, 519–522.
- Krs, M., Pruner, P. & Man, O. 2001: Tectonic and palaeogeographic interpretation of the paleomagnetism of Variscan and pre-Variscan formations of the Bohemian Massif, with special reference to the Barrandian Terrane. *Tectonophysics 332*, 93–114.
- Lenz, A.C. 1979: Llandoverian graptolite zonation in the northern Canadian Cordillera. *Acta palaeontologica polonica 24*, 137–153.
- Lenz, A.C. 1982. Llandoverian Graptolites of the Northern Canadian Cordillera: *Petalograptus*, *Cephalograptus*, *Rhaphidograptus*, *Dimorphograptus*, Retiolitidae, and Monograptidae. *Life Sciences Contributions*, *Royal Ontario Museum 130*, 1–154.
- Li Yanfang, Zhang Tongwei, Shao Deyong & Shen Baojian 2019: New U-Pb zircon age and carbon isotope records from the Lower Silurian Longmaxi Formation on the Yangtze Platform, South China: implications for stratigraphic correlation and environmental change. *Chemical Geology* 509, 249–260.
- Linnemann, U., Romer, R.L., Gehmlich, M. & Drost, K. 2004: Paläogeographic und Provenance des Saxothuringikums unter besonderer Beachtung der Geochronologie von prävariszischen Zirkonen und der Nd-Isotopie von Sedimenten. In: Linnemann, U. (ed), Das Saxothuringikum: Abriss der präkambrischen und paläozoischen Geologie von Sachsen and Thüringen. *Geologica Saxonica* 48/49, 121–132. [in German]
- Loydell, D.K. 2012: Graptolite biozone correlation charts. *Geological Magazine 149*, 1, 124–132. Loydell, D.K., Männik, P. & Nestor, V. 2003. Integrated biostratigraphy of the lower Silurian of the Aizpute-41 core, Latvia. *Geological Magazine 140*, 205–229.
- Loydell, D.K., Nestor, V. & Männik, P., 2010: Integrated biostratigraphy of the lower Silurian of the Kolka-54 core, Latvia. *Geological Magazine*, 147(2), 253-280.
- Loydell, D.K., Walasek, N., Schovsbo, N.H. & Nielsen, A.T. 2017: Graptolite biostratigraphy of the lower Silurian of the Sommerodde-1 core, Bornholm, Denmark. *Bulletin of the Geological Society of Denmark 65*, 135-160.
- Maletz, J., Wang, C.S., Kai, W. & Wang, X.F. 2021: Upper Ordovician (Hirnantian) to Lower Silurian (Telychian, Llandovery) graptolite biostratigraphy of the Tielugou section, Shennongjia anticline, Hubei Province, China. *Paläontologische Zeitschrift 95(3)*, 453–481. DOI 10.1007/s 12542-020-00544-5
- Manck, E. 1918: Die Graptolithen der Zone 18, sowie *Retiolites Eiseli* spec.nov., *Monogr. bispinosus* spec.nov. und *Diplograptus radiculatus* spec.nov. *Zeitschrift für Naturwissenschaften 86*, 337–344.

- Männik, P., Loydell, D.K., Nestor, V. & Nõlvak, J., 2015: Integrated Upper Ordovician–lower Silurian biostratigraphy of the Grötlingbo-1 core section, Sweden. *GFF 137(3)*, 226-244.Meidla, T., Tinn, O., Salas, M.J., Williams, M., Siveter, D., Vandenbroucke, T.R.A., Sabbe, K. 2013: Biogeographical patterns of Ordovician ostracods. In Harper, D.A.T. & Servais, T. (eds), Early Palaeozoic biogeography and palaeogeography. *Geological Society Memoirs 38*, 337–354.
- Melchin, M.J. 1989: Llandovery graptolite biostratigraphy and palaeobiogeography, Cape Phillips Formation, Canadian Arctic Islands. *Canadian Journal of Earth Science* 26, 1726–1746.
- Melchin, M.J. & Holmden, C. 2006: Carbon isotope chemostratigraphy of the Llandovery in Arctic Canada: Implications for global correlation and sea-level change. *GFF*, 128, 2, 173–180.
- Melchin, M.J. & MacRae, K.D. 2014. Insights into the Rhuddanian-Aeronian and Aeronian-Telychian boundary intervals from eastern and Arctic Canada. 86–88. *In Zhan Renbin & Huang Bing (eds): IGCP 591 Field Workshop 2014, Kunming China, Extended Summary*. Nanjing University Press, 246 pp.
- Melchin, M., Mitchell, C.E., Holmden, C. & Štorch, P. 2013: Environmental changes in the Late Ordovician early Silurian: Review and new insights from black shales and nitrogen isotopes. *The Geological Society of America Bulletin 125*, 1635–1670.
- Melchin, M.J., Cooper, R.A. & Sadler, P.M. 2004: The Silurian Period. *In* Gradstein, F.M. Ogg, J.G. & Smith, A.G. (eds.): *A Geologic Time Scale 2004*, 188-201. Cambridge University Press.
- Melchin, M. J., Sadler, P. M. & Cramer, B. D. 2012: The Silurian Period. 525-558. *In* Gradstein, F. M., Ogg, J. G. & Smith, A. G. (eds): *A Geologic Time Scale 2012*, Elsevier,
- Melchin, M.J., Sadler, P.M. & Cramer, B.D. 2020: The Silurian Period, 695–732. *In* Gradstein, F.M., Ogg, J.G., Schmitz, M.D. & Ogg, G.M. (eds): *Geologic Time Scale 2020*. Elsevier, Amsterdam. DOI 10.1016/B978-0-12-824360-2.00021-8
- Melchin, M.J., Boom, A., Davies, J. R., De Weirdt, J., McIntyre, A. J., Morgan, G., Phillips, S., Russell, C., Vandenbroucke, T. R.A., Williams, M. & Zalasiewicz, J. A. 2016: Integrated stratigraphic study of the Rhuddanian-Aeronian (Llandovery, Silurian) boundary succession at Rheidol Gorge, Wales. 60–61. *In* Guerdebeke, P., De Weirdt, J., Vandenbroucke, T. R. A. & Cramer, B. D. (eds), *IGCP 591 The Early to Middle Paleozoic Revolution, Closing Meeting, Ghent University, Belgium, 6–9 July 2016, Abstracts*, 134pp.
- Melchin, M.J., Davies, J.R., Boom, A., De Weirdt, J., McIntyre, A. J., Russell, C., Vandenbroucke, T. R.A. & Zalasiewicz, J. A. 2023: Integrated stratigraphical study of the Rhuddanian-Aeronian (Llandovery, Silurian) boundary succession in the Rheidol Gorge, Wales: a proposed Global Stratotype Section and Point for the base of the Aeronian Stage. *Lethaia* 56(1), 1 23. DOI 10.18261/let.56.1.8.
- Molyneux, S.G., Delabroye, A., Wicander, R., Servais, T. 2013: Biogeography of early to mid Palaeozoic (Cambrian–Devonian) marine phytoplankton. In Harper, D.A.T. & Servais, T. (eds), Early Palaeozoic biogeography and palaeogeography. *Geological Society Memoirs 38*, 365–397.
- Murphy, J.B., Gutiérrez-Alonso, G., Nance, R.D., Fernandez-Suarez, J., Keppie, J.D., Quesada, C., Strachan, R.A. & Dostal, J. 2006: Origin of the Rheic Ocean: rifting along a Neoproterozoic suture? *Geology 34*, 325–328.
- Nestor, V., 1980. Middle Llandoverian chitinozoans from Estonia. *Proceedings of the Estonian Academy of Sciences, Geology* 29, 131–142.

- Nestor, V., 1994. Early Silurian chitinozoans of Estonia and North Latvia. *Academia* 4, 163 pp.
- Nestor, V., 1999. Distribution of chitinozoans in the Llandovery of the Oslo region. *Bollettino-Societa Paleontologica Italiana* 38(2/3), 227-238.
- Ni Yunan 1978: Lower Silurian graptolites from Yichang, western Hubei. *Acta Palaeontologica Sinica* 17, 387–420. [in Chinese with English Abstract]
- Obut, A.M. & Sennikov, N.V. 1985: Graptolite zones in the Ordovician and Silurian of the Gorny Altai. In Hughes, C.P. & Rickards, R.B. (eds): Palaeoecology and Biostratigraphy of Graptolites. *Geological Society Special Publication* 20, 155–164.
- Obut, A.M., Sobolevskaya, R.F. & Merkureva, A.P. 1968: Graptolity Llandoveri v kernakh burovykh skvazhin Norilskogo rayona. 162 pp. Akademia nauk USSR, Sibirskoe ottdelenie. Institut geologii i geofyziki, Moskva. [in Russian]
- Oczlon, M. 1992: Examples of Palaeozoic contourites, tempestites, and turbidites classification and palaeogeographic approach. *Heidelberger Geowissenschaftliche Abhandlungen 53*, 57–159.
- Paris, F., Miller, M.A. & Zalasiewicz, J. 2015: Early Silurian chitinozoans from the Qusaiba type area, north Central Saudi Arabia. *Review of Palaeobotany and Palynology 212*, 127-186.
- Paris, F., Verniers, J., Al-Hajri, S. & Al-Tayyar, H. 1995: Biostratigraphy and palaeogeographic affinities of Early Silurian chitinozoans from central Saudi Arabia. *Review of Palaeobotany and Palynology* 89(1-2), 75-90.
- Paškevičius, J. 1979: *Biostratigraphy and graptolites of the Lithuanian Silurian*. 267pp., Mosklas, Vilnius. [in Russian]
- Patočka, F., Pruner, P. & Štorch, P. 2003: Palaeomagnetism and geochemistry of Early Palaeozoic rocks of the Barrandian (Teplá–Barrandian Unit, Bohemian Massif): palaeotectonic implications. *Physics and Chemistry of the Earth 28*, 735–749.
- Přibyl, A. 1937: O stratigrafických poměrech vrstev želkovických eα1 u Hlásné Třebaně. *Věstník Státního geologického ústavu 13*, 4.
- Ray, D.C. (ed.) 2011: Siluria Revisited: A Field Guide. International Subcommission on Silurian Stratigraphy, Field Meeting 2011, 170pp.
- Robardet, M. 2003: The Armorica microplate: fact or fiction? Critical review of the concept and contradictory palaeobiogeographical data. *Palaeogeography, Palaeoclimatology, Palaeoecology* 195, 25–148.
- Salvador, A. (ed.) 1994: *International Stratigraphic Guide*, 2nd ed. Boulder: IUGS and Geological Society of America, 214pp.
- Schauer, M. 1971: Biostratigraphie und Taxionomie der Graptolithen des tieferen Silurs unter besonderer Berücksichtigung der tektonischen Deformation. *Freiberger Forschungshefte Reihe C 373*, 1–185.
- Sennikov, N.V. 1976: Graptolites and Lower Silurian Stratigraphy of the Gorny Altai. Nauka Press, Moskva, 274 pp. [in Russian]
- Sennikov N.V., Yolkin E.A., Petrunina Z.E., Gladkikh L.A., Obut O.T., Izokh N.G. & Kipriyanova T.P., 2008: *Ordovician-Silurian Biostratigraphy and Paleogeography of the Gorny Altai*. SB RAS Publishing House, Novosibirsk, 156 p. [in Russian]
- Stampfli, G.M., von Raumer, J. & Borel, G.D. 2002: Paleozoic evolution of pre-Variscan terranes: from Gondwana to the Variscan collision. In Martínez Catalán, J.R., Hatcher, R.D. Jr., Arenas,

- R., Díaz García, F. (eds), Variscan-Appalachian Dynamics: The Building of the Late Paleozoic Basement. Special Papers-Geological Society of America 364, 263–280.
- Štorch, P. 1986: Ordovician-Silurian boundary in the Prague Basin (Barrandian area, Bohemia). Sborník geologických Věd, Geologie 41, 69–103.
- Štorch, P. 1991: Faciální vývoj, stratigrafie a korelace svrchního ordoviku a spodního siluru pražské pánve (Barrandien). *Unpublished PhD Thesis*, 232 pp., Czech geological Survey, Prague. [in Czech]
- Štorch, P. 1994: Graptolite biostratigraphy of the Lower Silurian (Llandovery and Wenlock) of Bohemia. *Geological Journal* 29, 137–165.
- Štorch, P. 1996: The basal Silurian *Akidograptus ascensus Parakidograptus acuminatus* Biozone in peri-Gondwanan Europe: graptolite assemblages, stratigraphical ranges and palaeobiogeography. *Bulletin of the Czech Geological Survey* 71, 171–178.
- Štorch, P. 1998: Graptolites of the *Pribylograptus leptotheca* and *Lituigraptus convolutus* biozones of Tmaň (Silurian, Czech Republic). *Journal of the Czech Geological Society* 43, 209–272.
- Štorch, P. 2006: Facies development, depositional settings and sequence stratigraphy across the Ordovician-Silurian boundary: a new perspective from Barrandian area of the Czech Republic. *Geological Journal* 41, 163–192.
- Štorch, P. 2015: Graptolites from Rhuddanian-Aeronian boundary interval (Silurian) in the Prague Synform, Czech Republic. *Bulletin of Geosciences* 90, 841 891.
- Štorch, P. 2023: Graptolite biostratigraphy and biodiversity dynamics in the Silurian System of the Prague Synform (Barrandian area, Czech Republic). *Bulletin of Geosciences* 98(1), 1–78.
- Štorch, P. & Frýda, J. 2012: The late Aeronian graptolite sedgwickii Event, associated positive carbon isotope excursion and facies changes in the Prague Synform (Barrandian area, Bohemia). *Geological Magazine 149*, 1089–1106.
- Štorch, P. & Melchin, M.J. 2018: Lower Aeronian triangulate monograptids of the genus *Demirastrites* Eisel, 1912: biostratigraphy, paleobiogeography, anagenetic changes and speciation. *Bulletin of Geosciences 93 (4)*, 513-537.
- Štorch, P., Manda, Š., Tasáryová, Z., Frýda, J., Chadimová, L. & Melchin, M.J. 2018: A proposed new global stratotype for Aeronian Stage of the Silurian System: Hlásná Třebaň section, Czech Republic. *Lethaia* 51(3), 357–388. DOI 10.1111/let.12250
- Štorch, P. & Kraft, P. 2009: Graptolite assemblages and Stratigraphy of the lower Silurian Mrákotín Formation, Hlinsko Zone, NE interior of the Bohemian Massif (Czech Republic). *Bulletin of Geosciences* 84, 51-74.
- Štorch, P. & Massa, D. 2003: Biostratigraphy, Correlation, Environmental and Biogeographic Interpretation of the Lower Silurian Graptolite Faunas of Libya. *In Salem, M.J. & Oun, K.M.* (eds), The Geology of Northwest Libya, Vol. 1, 237-251.
- Strauss, J.V., Fraser, T., Melchin, M.J., Allen, TJ., Malinowski, J., Feng, X., Taylor, J.F., Day, J., Gill, B.C. & Sperling, E.A. 2020: The Road River Group of northern Yukon: Early Paleozoic deep-water sedimentation with the Great American Carbonate Bank: Supplementary Material. *Canadian Journal of Earth Sciences* 57, cjes-2020-0017 suppla.pdf.
- Sudbury, M. 1958: Triangulate monograptids from the *Monograptus gregarius* Zone (Lower Llandovery) of the Rheidol Gorge (northern Cardiganshire). *Philosophical Transactions of the Royal Society of London, Series B 241*, 485–555.

- Tait, J., Bachtadse, V. & Soffel, H.C. 1994: Silurian palaeogeography of Armorica new palaeomagnetic data from Central Bohemia. *Journal of Geophysical Research: Solid Earth* 99, 2897–2907.
- Tait, J., Bachtadse, V. & Soffel, H.C. 1995: Upper Ordovician palaeogeography of the Bohemian Massif implications for Armorica. *Geophysical Journal International* 122, 211–218.
- Tasáryová, Z., Schnabl, P., Čížková, K., Pruner, P., Janoušek, V., Rapprich, V., Štorch, P., Manda, Š., Frýda, J. & Trubač, J. 2014: Gorstian palaeoposition and geotectonic setting of Suchomasty Volcanic Centre (Silurian, Prague Basin, Teplá–Barrandian Unit, Bohemian Massif). *GFF* 136, 262–265.
- Temple, J.T. 1988: Biostratigraphical correlation and stages of the Llandovery. *Journal of the Geological Society of London 145*, 875–879.
- Toghill, P. 1968: The graptolite assemblages and zones of the Birkhill Shales (Lower Silurian) at Dobb's Linn. *Palaeontology* 11, 654–668.
- Torsvik, T.H. & Cocks, L.R.M. 2013: New global palaeogeographical reconstructions for the Early Palaeozoic and their generation. In Harper, D.A.T. & Servais, T. (eds), Early Palaeozoic Biogeography and Palaeogeography. *Geological Society, London, Memoirs* 38, 5–24.
- Verniers, J., Nestor, V., Paris, F., Dufka, P., Sutherland, S. & Van Grootel, G. 1995: A global Chitinozoa biozonation for the Silurian. *Geological Magazine 132(6)*, 651–666.
- Vodička, J. & Butcher, A. 2023. Chitinozoans of the GSSP candidate for the Rhuddanian-Aeronian (Silurian) boundary in the Hlásná Třebaň (Prague Basin, Czech Republic). 4th International Congress on stratigraphy Strati2023, Lille, France. Book of Abstracts, 318-319.
- von Raumer, J. & Stampfli, G.M. 2008: The birth of the Rheic Ocean Early Palaeozoic subsidence patterns and subsequent tectonic plate scenarios. *Tectonophysics* 461, 9–20.
- Waern, B. 1960: On the Middle Llandovery of Dalarne. Reports of 21 Session, International. Geological Congress. Norden, Copenhagen Section 7, 126–133.
- Wang Xiaofeng 1985: Lower Silurian graptolite zonation in the eastern Yangzi (Yangtze) Gorges, China. *Bulletin of the Geological Society of Denmark 35*, 231–243.
- Wignall, P.B. 1994: Black shales. Oxford University Press, Oxford, 127 pp.
- Wignall, P.B. & Twitchett, R.J. 1996: Oceanic anoxia and the end of Permian mass extinction. *Science*, 272. 1155–1158.
- Wignall, P.B., Newton, R. & Brookfield, M.E. 2005: Pyrite framboid evidence for oxygen-poor deposition during the Permian-Triassic crisis in Kashmir. *Palaeogeography, Palaeoclimatology, Palaeoecology 216*, 183–188.
- Wilkin, R.T., Barnes, H.I. & Brantley, S.I. 1996: The size distribution of framboidal pyrite in modern sediments as indicator of redox conditions. *Geochimica et Cosmochimica Acta 60*, 3897–3912.
- Zalasiewicz, J.A. & Tunnicliff, S. 1994: Uppermost Ordovician to lower Silurian graptolite biostratigraphy of the Wye Valley, central Wales. *Palaeontology* 37(3), 695–720.
- Zalasiewicz, J.A., Taylor, L., Rushton, W.A., Loydell, D.K., Rickards, R.B. & Williams, M. 2009: Graptolites in British stratigraphy. *Geological Magazine 146*, 785–850.